Title:

Multifunctional requirements for ERK1/2 signaling in the development of ganglionic eminence derived glia and cortical inhibitory neurons

Author Names and Affiliations:

Sara J. Knowles[1], Michael C. Holter[1], Guohui Li[2], George R. Bjorklund[1], Katherina P. Rees[1], Johan S. Martinez-Fuentes[1], Kenji J. Nishimura[1], Ariana E. Afshari[1], Noah Fry[1], April M Stafford[3], Daniel Vogt[3], Marco Mangone[4], Trent Anderson[2], and Jason M. Newbern[1,*]

[1] School of Life Sciences, Arizona State University; Tempe, AZ 85287, USA

[2] College of Medicine, University of Arizona, Phoenix, AZ 85004, USA

[3] Department of Pediatrics and Human Development, Michigan State University, Grand Rapids, MI 49503, USA

[4]Virginia G. Piper Center for Personalized Diagnostics, The Biodesign Institute at Arizona State University, 1001 S McAllister Ave, Tempe, AZ 85281, USA.

*Corresponding Author address:

School of Life Sciences, PO Box 84501

Arizona State University

Tempe, AZ 85287-4501, USA

jason.newbern@asu.edu

Abstract

The RAS/RAF/MEK/ERK1/2 intracellular signaling pathway is activated by numerous cues during brain development and dysregulated in neurodevelopmental syndromes, particularly the RASopathies and certain forms of autism. Cortical excitatory/inhibitory imbalance is thought to be critical in the neuropathogenesis of these conditions. However, the developmental functions of ERK1/2 signaling in cortical inhibitory neurons (CINs) and other medial ganglionic eminence (MGE)-derived non-neuronal cells are poorly understood. Here, we genetically modulated ERK1/2 signaling in mouse MGE neural progenitors or GABAergic neurons in vivo. We find that MEK-ERK1/2 signaling is essential for regulating MGE-derived oligodendrocyte number in the anterior commissure. While *Erk1/2* inactivation does not alter CIN number, we show that CIN-autonomous ERK1/2 signaling is necessary for chemogenetic activity-dependent FOSB expression in vivo. This deficit coincides with a significant and persistent reduction in somatostatin, but not parvalbumin, expression in a subset of ERK1/2 deleted inhibitory neurons. Interestingly, one week of chronic chemogenetic stimulation in juvenile or adult animals partially rescues the decrease in somatostatin expression in *Erk1/2* mutant CINs. Our data demonstrate ERK1/2 signaling is required for the establishment of MGE-derived glia, whereas in CINs, ERK1/2 drives activity dependent-responses and the expression of somatostatin in a subset of neurons.

Introduction

The canonical RAS/RAF/MEK/ERK1/2 intracellular kinase cascade is a ubiquitous pathway activated by a wide array of extracellular signals (Lavoie et al., 2020). Mutations in Receptor Tyrosine Kinase (RTK)-associated effectors and upstream regulators of Extracellular Regulated Kinase (ERK1/2, aka *MAPK3/1*) signaling cause a family of developmental syndromes collectively termed the "RASopathies" (Rauen, 2013). Individuals with RASopathies frequently exhibit craniofacial abnormalities, cardiac malformations, and increased cancer risk, in addition to neurological conditions such as epilepsy, developmental delay, intellectual disability, and autism (Tidyman & Rauen, 2016). Most RASopathy mutations increase ERK1/2 signaling, however, microdeletions that disrupt *Erk1* or *Erk2* expression have been linked to neurocognitive delay (Ben-Shachar et al., 2008; Fernandez et al., 2010; Linhares et al., 2016; Newbern et al., 2008; Nowaczyk et al., 2014; Pucilowska et al., 2015; Rauen, 2013; Saitta et al., 2004; Samuels et al., 2009; Sánchez et al., 2020). Moreover, ERK1/2 signaling is a point of functional convergence for several autism and schizophrenia-associated copy number variants (Blizinsky et al., 2016; Courchesne et al., 2020; Heavner & Smith, 2020; Lord et al., 2020; Moyses-Oliveira et al., 2020; Rosina et al., 2019). Understanding the normal functions of ERK1/2 signaling in the developing forebrain may be instructive for defining neuropathological mechanisms in multiple neurodevelopmental syndromes.

The patterning of the forebrain is heavily dependent upon canonical trophic cues known to activate RTK signaling, but the precise functions of downstream kinase cascades are less clear (Assimacopoulos et al., 2003; Faedo et al., 2010; Maisonpierre et al., 1990; O'Leary et al., 2007). Studies of the mouse dorsal pallium have shown that FGF and ERK1/2 signaling via

ETV5 are crucial for cortical gliogenesis, while neurogenesis is relatively less affected (Dinh Duong et al., 2019; Fyffe-Maricich et al., 2011; S. Li et al., 2014; X. Li et al., 2012; Pucilowska et al., 2012). Interestingly, cell-specific *Mek1/2*-deletion in embryonic cortical excitatory neurons leads to subtype-specific deficits in morphological and electrophysiological properties during the early postnatal period (L. Xing et al., 2016). In contrast to mouse excitatory neurons, GABAergic cortical inhibitory neurons (CINs) are primarily derived from progenitor domains in the medial and caudal ganglionic eminences (MGE and CGE) (Wonders & Anderson, 2006). CIN patterning cues, migratory paths, master transcription factors, and expression levels of ERK1/2 pathway components differ significantly from dorsally derived glutamatergic neurons (Mardinly et al., 2016; Mayer et al., 2018; Ryu, Kang, et al., 2019; Ryu, Kim, et al., 2019; Talley et al., 2021). It is unknown whether ERK1/2 signaling has similar or unique functions in the development of glial and neuronal derivatives of the ganglionic eminences.

CINs exhibit substantial heterogeneity in their morphology, gene expression profile, electrophysiological properties, and contributions to cognition (Bomkamp et al., 2019; DeFelipe et al., 2013; Gour et al., 2021; Lim et al., 2018; Mayer et al., 2018; Petros et al., 2015). The two largest classes of CINs are defined by parvalbumin (PV) or somatostatin (SST) expression and are distinguished by unique electrophysiological properties (Dehorter et al., 2015; Lim et al., 2018; Okaty et al., 2009; Pan et al., 2018; Urban-Ciecko & Barth, 2016). Differences in their generation and local morphogen gradients bias progeny towards specific subtypes (McKenzie et al., 2019; Miyoshi et al., 2007; Petros et al., 2015). Trophic cues and neurotransmitters (ex. BDNF/TrkB, Neuregulin-1/ErbB4, glutamate/NMDAR) are also important extracellular influences on CIN development (Cancedda et al., 2007; De Marco

García et al., 2011; Exposito-Alonso et al., 2020; Fazzari et al., 2010; Glorioso et al., 2006; Hong et al., 2008; Huang et al., 1999; Itami et al., 2007; Miller et al., 2011). While the transcriptional mechanisms of CIN development have been intensely studied, the signaling pathways that serve as intermediaries between extracellular stimulation and gene expression changes are relatively less clear. Recent work has shown that hyperactive MEK-ERK1/2 and PI3K-linked signaling pathways have critical roles in CIN development and subtype specification (Angara et al., 2020; Malik et al., 2019; Vogt et al., 2015). However, the field still lacks crucial information on whether activation of ERK1/2 signaling is necessary for CIN subtype identity.

The initial stages of postnatal development are characterized by a series of activity-dependent events in which CINs play a critical role (Ben-Ari et al., 2007; Cancedda et al., 2007; Close et al., 2012; Denaxa et al., 2012). Early spontaneous activity causes the release of GABA, which functions as a neurotransmitter and trophic cue to depolarize neurons and promote connections in the nascent cortical circuit (Ben-Ari et al., 2007; Owens & Kriegstein, 2002). Later stages of patterned activity are especially important for establishing the timing of critical periods and excitatory/inhibitory tone in cortical networks (Reh et al., 2020). Activity-dependent responses have been well studied in cortical excitatory neurons, where glutamatergic activation of ERK1/2 has been shown to modulate synaptic strength (Cristo et al., 2001; Thomas & Huganir, 2004; Wu et al., 2001; J. Xing et al., 1996; Yap & Greenberg, 2018). CINs express different levels of glutamate receptor subunits, calcium-binding proteins, and calcium responsive kinases that modulate intracellular signaling responses to glutamate (Cohen et al., 2016; Matthews et al., 1994; Paul et al., 2017; Sik et al., 1998; Tasic et al., 2016; Topolnik, 2012). Indeed, many features of the activity-dependent transcriptome in CINs

differ from excitatory neurons (Guenthner et al., 2013; Hrvatin et al., 2018; Mardinly et al., 2016; Spiegel et al., 2014). Nonetheless, the phosphorylation-dependent signaling requirements for ERK1/2 in CINs are difficult to assess with transcriptomic approaches.

Studying the functions of ERK1/2 specifically in ventral forebrain derivatives using germline knockouts of *Erk1* and *Erk2* is complicated by a combination of embryonic lethality, compensatory interactions, and non-cell autonomous effects (Newbern et al., 2011; Samuels et al., 2008; Selcher, 2001). Therefore, we used cell-specific genetic modifications in embryonic mice to conditionally inactivate ERK1/2 signaling in medial ganglionic eminence (MGE) progenitors (*Nkx2.1*^{Cre}) and GABAergic neurons (*VGAT*^{Cre}). We show that ERK1/2 signaling is a critical modulator of MGE-derived oligodendrocyte number in juvenile mice. In contrast, ERK1/2 appears dispensable for early expression of core GABAergic genes and global CIN number. Further analysis of postnatal stages of cortical maturation revealed that the expression of SST protein in a subset of CINs requires ERK1/2 signaling. We also found that ERK1/2 is vital for activity-dependent FOSB expression in CINs following chemogenetic stimulation in vivo. Moreover, chronically increasing CIN activity during early postnatal stages or in adulthood was sufficient to partially rescue SST expression. Our data reveal previously undescribed roles for ERK1/2 signaling in select aspects of ventral forebrain glial development and the maturation of CINs. These results may also inform our understanding of the cellular events underlying neurodevelopmental disorders linked to aberrant ERK1/2 signaling.

Results

ERK1/2 signaling regulates the number of ventral forebrain-derived oligodendrocytes.

The ERK1/2 signaling pathway is an established regulator of dorsal pallium derived glial number, but its role in glial specification from subpallial progenitor domains remains less clear (Dinh Duong et al., 2019; X. Li et al., 2012). Neural progenitors within the subpallial medial ganglionic eminence (MGE) produce both neurons and glia after regional patterning by the transcription factor *Nkx2.1* at ~E8.5 (Shimamura & Rubenstein, 1997). *Nkx2.1*^{Cre} mice provide a valuable tool to selectively induce genetic modifications in MGE-derived glia and cortical inhibitory neurons (CINs) early in development. To completely inhibit ERK1/2 signaling and fluorescently label MGE derivatives, we generated quadruple genetically modified mice with germline *Erk1*/*Mapk3* deletion (*Erk1*$^{-/-}$), loxp-flanked ("floxed") *Erk2/Mapk1* exon 2 alleles (*Erk2*$^{fl/fl}$), *Nkx2.1*$^{Cre\ +/-}$, and a Cre-dependent tdTomato/RFP reporter, *Ai9*$^{+/-}$ (see *Genetically modified mice* in Materials and Methods) (Madisen et al., 2010; Newbern et al., 2008; Samuels et al., 2008; Selcher, 2001; L. Xing et al., 2016; Xu et al., 2008). *Nkx2.1*^{Cre}, *Ai9* mice showed a pattern of RFP-labeled neurons and glia consistent with previous reports (**Figure1A**, **Figure 1-figure supplement 1A**) (Madisen et al., 2010; Xu et al., 2008). Mutant mice with complete *Nkx2.1*^{Cre}-mediated *Erk1/2* inactivation (*Erk1*$^{-/-}$, *Erk2*$^{fl/fl}$, *Nkx2.1*^{Cre}, *Ai9*) were born at normal Mendelian ratios, survived into adulthood, and exhibited a significant reduction in ERK2 protein in CINs and ventral glia (**Figure 1- figure supplement 1C-N**).

The anterior commissure is a ventral white matter tract populated by glia from multiple progenitor domains including the MGE (Kessaris et al., 2006; Minocha et al., 2015). We used a marker of the oligodendrocyte lineage, OLIG2, to quantify the density of oligodendrocytes at postnatal day 14 (P14). We found a significant reduction in OLIG2^{+}/RFP^{+} co-expressing cells in

the anterior commissure of *Erk1*$^{-/-}$, *Erk2*$^{fl/fl}$, *Nkx2.1*^{Cre}, *Ai9* mutants when compared with *Erk1*$^{-/-}$, *Erk2*$^{fl/wt}$, *Nkx2.1*^{Cre}, *Ai9* littermate controls (CTL 473 +/- 34 cells/mm^2, MUT 13 +/- 13 cells/mm^2, *p*=.0002, student's t-test) (**Figure 1B-H**, **Figure 1- figure supplement 1B**). GFAP$^+$/RFP$^+$ astrocyte density was similarly reduced (CTL 84 +/- 9 cells/mm^2, MUT 19 +/- 9 cells/mm^2, *p*=.016, student's t-test) (data not shown), suggesting that ERK1/2 signaling is necessary for MGE-derived astrocyte and oligodendrocyte number.

RASopathies are primarily caused by mutations that hyperactive ERK1/2, and often other, signaling cascades. To determine if hyperactive MEK-ERK1/2 signaling is sufficient to modulate MGE-derived glial density in the ventral forebrain, we generated mice expressing a Cre-dependent hyperactivating *Mek1*$^{S217/221E}$ mutation (*CAG-loxpSTOPloxp-Mek1*$^{S217/221E}$*)*. *Mek1*$^{S217/221E}$, *Nkx2.1*^{Cre}, *Ai9* mutants display increased MEK1 levels in RFP$^+$ CINs and glia (**Figure 1 -figure supplement 1O-Z**) (Alessi et al., 1994; Bueno, 2000; Cowley, 1994; Holter et al., 2021; Klesse et al., 1999; Krenz et al., 2008; Lajiness et al., 2014; X. Li et al., 2012). In contrast to *Erk1/2* inactivation, *Mek1*$^{S217/221E}$, *Nkx2.1*^{Cre}, *Ai9* mutants showed an increase in OLIG2$^+$/RFP$^+$ cell density in the anterior commissure at P21 compared with *Nkx2.1*^{Cre}, *Ai9* littermate controls (WT 285 +/- 74 cells/mm^2, *Mek1*$^{S217/221E}$ 692 +/- 51 cells/mm^2, *p*=.004, student's t-test) (**Figure 1I-M**, **Figure 1- figure supplement 1B**). In addition, we observed ectopic MGE-derived glial profiles in the fimbria of *Mek1*$^{S217/221E}$, *Nkx2.1*^{Cre}, *Ai9* mutants (**Figure 1N-R**). These data indicate that increased MEK-ERK1/2 signaling enhances MGE-derived oligodendrocyte number.

Reduced ERK1/2 signaling does not alter total CIN number in the somatosensory cortex.

ERK1/2 signaling is necessary for the survival and physiological maturation of select excitatory neuron subpopulations, but its requirement for CIN development is unclear (L. Xing et al., 2016). In the primary somatosensory cortex of *Erk1*$^{-/-}$, *Erk2*$^{fl/fl}$, *Nkx2.1*^{Cre}, *Ai9* mice, we found no difference in the density of Cre-recombined cells compared with controls at P14 (**Figure 2A-E**, p=0.476, student's t-test) and P60 (p=0.288, student's t-test) (data not shown). *Nkx2.1*^{Cre} does not recombine in the fraction of CINs derived from the lateral or caudal ganglionic eminences (Kessaris et al., 2006; Talley et al., 2021). These data suggest ERK1/2 is not required for the generation of the subset of CINs derived from the MGE.

To comprehensively assess the role of *Erk1/2* in all postmitotic GABAergic neurons, we generated conditional mutants using *VGAT/Slc32a1*^{Cre} (**Figure 2- figure supplement 1A-G**) (Madisen et al., 2010; Vong et al., 2011). *VGAT*^{Cre} is expressed in all GABAergic neurons early in development. We found that *Erk1*$^{-/-}$, *Erk2*$^{fl/fl}$, *VGAT*^{Cre}, *Ai9* mutant mice were born at normal Mendelian ratios but exhibited profound growth delay by the end of the first postnatal week and lethality in the second (n=10). No significant difference in the density of RFP^{+} cells was observed between P5 *Erk1*$^{-/-}$, *Erk2*$^{fl/fl}$, *VGAT*^{Cre}, *Ai9* mutant and *Erk1*$^{-/-}$, *Erk2*$^{fl/wt}$, *VGAT*^{Cre}, *Ai9* control cortices (CTL 998 +/- 98 cells/mm^2, MUT 1010 +/- 162 cells/mm^2, p=.955, student's t-test) (**Figure 2F-J**). Qualitatively similar results were obtained in a separate line using *Dlx5/6*^{Cre}, which also targets postmitotic GABAergic neurons in the cortex (**Figure 2- figure supplement 1H-K**) (Monory et al., 2006). Together, these data suggest that ERK1/2 signaling is dispensable for the initial establishment and maintenance of CIN number.

ERK1/2 deletion alters the maturation of a subset of SST neurons.

CINs are a heterogeneous population of neurons that can be divided into numerous subtypes with overlapping but distinct transcriptional profiles. Although CIN number was unaltered in the cortex following ERK1/2 deletion, gene expression in these cells remained unknown. To study the CIN translatome, we employed a Cre-dependent 'Ribotag' mouse that expresses an HA-fused ribosomal protein, $RPL22^{HA}$, for translating ribosome affinity purification followed by RNA sequencing (Sanz et al 2009). Whole cortices were dissected from P7.5 $Erk1^{-/-}$, $Erk2^{fl/fl}$, $VGAT^{Cre}$, $Rpl22^{HA}$ (MUT), $Erk1^{-/-}$, $Erk2^{fl/wt}$, $VGAT^{Cre}$, $Rpl22^{HA}$ (HET), or wild type controls ($Erk1^{+/+}$, $Erk2^{wt/wt}$, $VGAT^{Cre}$, $Rpl22^{HA}$) (WT). Following homogenization, HA-containing ribosomes were immunoprecipitated and RNA was purified from cortical (INPUT) or immunoprecipitated (IP) samples, amplified, and sequenced. As expected, we observed a near complete absence of reads complementary to *Erk1/Mapk3* exons 1-6 in $Erk1^{-/-}$ animals and a gene dose dependent reduction of *Erk2/Mapk1* exon 2 in IP fractions (**Figure 3- figure supplement 1A**). A comparison of the >3400 differentially expressed genes between IP and INPUT fractions within each genotype revealed that IP fractions exhibited significant enrichment of *Cre* and well-established core GABAergic genes (*Gad1/2*, *Slc32a1*, *Erbb4*, *Dlx1/2/5/6*), as well as significant depletion of genes expressed in glia (*Fabp7, Sox10, Pdgfra, S100b*) and excitatory neurons (*Neurod1/6, Camk2a*) (**Table S1** and **Figure 3- figure supplement 1B-C**) (Hrvatin et al., 2018; Mardinly et al., 2016; Mi et al., 2018; Paul et al., 2017; Tasic et al., 2016). These data indicate the Ribotag approach significantly enriched samples for CIN-derived mRNA.

We next examined the differential expression of genes between control (HET) and mutant (MUT) IP, CIN-enriched samples, particularly those important for GABAergic specification and subtype identity. A significant decrease in known ERK1/2 target genes *Spry4*, *Etv5*, and *Egr2* was noted in MUT IP samples (**Figure 3A-magenta**) (X. Li et al., 2012; Newbern et al., 2011;

L. Xing et al., 2016). However, the expression of master transcriptional regulators of global CIN identity (*Lhx6, Dlx2/5/6)* and GABAergic metabolism *(Gad1/2, Slc32a1*) was not significantly different between HET and MUT IP samples (**Figure 3A-green**). GO analysis detected a significant overrepresentation of differentially expressed genes in the category of "regulation of cell differentiation" (GO:0045595, adj. p =.002) and "nervous system development" (GO:0030182, adj. p =.04). Indeed, we observed changes in the expression of genes linked to neural maturation (*Notch1, Smo, Fgf18, Bdnf*) and CIN subtype specification (*Mafb, Sst, Sp9, Crhbp, Grin2d*). Together, these data indicate that ERK1/2 inactivation does not significantly disrupt core mediators of CIN identity but may have selective effects on later stages of subtype maturation.

We further analyzed CIN subtypes in *Erk1*$^{-/-}$, *Erk2*$^{fl/fl}$, *VGAT*^{Cre}, *Ai9* brains at P5, prior to the typical period of lethality. At this stage SST, a canonical marker of a subset of regular spiking (RS) CINs, and Calbindin 1 (CALB1), a calcium binding protein co-expressed in a subset of CINs partially overlapping with SST, are expressed (Forloni et al., 1990; Marsh et al., 2016; Martin et al., 2017; Mi et al., 2018; Munguba et al., 2019; Nigro et al., 2018; Tasic et al., 2016). We assessed these two classes of SST^{+} CINs and found a statistically significant reduction in SST^{+}/CALB1^{-} cells in mutants relative to littermate controls (p=0.017, student's t-test), but no change in SST^{+}/CALB1^{+} co-expressing cells (p=0.938, student's t-test) (**Figure 3B-J**). The early lethality of the *Erk1*$^{-/-}$, *Erk2*$^{fl/fl}$, *VGAT*^{Cre}, *Ai9* mice prohibited our ability to study fully mature CIN markers, as PV is not expressed until the second postnatal week and only a subset of RS CINs have initiated SST protein expression (del Rio et al., 1994; Huang et al., 1999). Nonetheless, our data are consistent with a role for ERK1/2 in the early development of SST-CIN subtypes in the first postnatal week.

The broad recombination pattern of *VGAT*^{Cre} throughout the entire nervous system leaves open the possibility of systemic, non-cell-autonomous effects on CIN development. We therefore performed more detailed studies of subtype specification in *Nkx2.1*^{Cre} mutants, where recombination occurs in a smaller subset of CINs, but survival extends into adulthood. Quantification of PV-CIN number in P14 and adult *Erk1*$^{-/-}$, *Erk2*$^{fl/fl}$, *Nkx2.1*^{Cre}, *Ai9* mice revealed no differences in the proportion of PV-CINs or their somal size (**Figure 4A-R**). Notably, we observed a significant reduction in the proportion of SST-CINs at P14, a trend which persisted into adulthood (**Figure 4A-Q**). This phenotype presumably requires complete loss of ERK1/2 signaling since *Erk2*$^{fl/fl}$, *Nkx2.1*^{Cre} mutants showed no difference in the density of SST-CINs at P30 (**Figure 4- figure supplement 1A-E**). Attempts to generate an *Erk1*$^{-/-}$, *Erk2*$^{fl/fl}$, *SST*^{Cre} strain yielded no viable mutants at birth (0 of 49, 12 expected) (Taniguchi et al., 2011). Hyperactivation of MEK-ERK1/2 signaling in P21 *Mek1*$^{S217/221E}$, *Nkx2.1*^{Cre}, *Ai9* mice did not alter the density of SST-CINs, though we observed the previously reported decrease in GABAergic neuron number due to embryonic loss of PV-CINs (**Figure 4- figure supplement 1F-J**) (Holter et al., 2021). Together, these data demonstrate subtype-selective requirements for ERK1/2 signaling in regulating SST expression.

ERK1/2 regulates activity-dependent FOSB expression in CINs following chemogenetic depolarization.

The postnatal maturation of CINs is dependent on trophic cues and neurotransmitter signaling. NRG1/ERBB4, BDNF/TRKB, and glutamate/NMDAR signaling promote appropriate activity-dependent responses in CINs through the activation of multiple intracellular signaling cascades (Fazzari et al., 2010; Huang et al., 1999; Ting et al., 2011; Yap & Greenberg, 2018).

However, the specific roles of ERK1/2 signaling in this process remain unclear. To interrogate the cell-autonomous contributions of ERK1/2 to CINs' activity-dependent gene expression we directly activated a subpopulation of GABAergic neurons using a chemogenetic approach with Designer Receptors Exclusively Activated by Designer Drugs (DREADDs). DREADDs are based on a modified G-Protein-Coupled Receptor and the engineered ligand, clozapine-*N*-oxide (CNO) (Jendryka et al., 2019; Nawaratne et al., 2008; Roth, 2016). In hM3D$_q$-DREADD expressing neurons, CNO has been shown to activate G$_q$-PLC signaling, resulting in KCNQ channel closure, TRPC channel opening, and ultimately membrane depolarization (Choveau et al., 2012; Mori et al., 2015; Rogers et al., 2021; Roth, 2016; Topolnik et al., 2006; Zou et al., 2016).

We generated *Erk1*$^{-/-}$, *Erk2*$^{fl/fl}$, *Nkx2.1*^{Cre}, *G*$_q$*-DREADD-HA* animals for chemogenetic activation of CINs (Rogan & Roth, 2011; Zhu et al., 2016). We performed patch-clamp recordings in acute slices from P15-P22 cortices and found bath application of 10µM CNO induced a depolarizing increase in the holding current of both control and ERK1/2 inactivated CINs (p<.05, paired t-test) (**Figure 5A**). Current clamp recordings revealed that depolarizing current injections following application of CNO significantly increased firing frequency when compared to baseline conditions (p<.05, paired t-test) (**Figure 5B**). We next examined the intrinsic electrophysiological properties of neurons with a fast-spiking (FS) phenotype (**Figure 5C**) (Anderson et al., 2010; Kawaguchi, 1997; McCormick et al., 1985). We did not detect a difference in resting membrane potential (CTL -69.00 ± 1.8 mV, MUT -69.75 ± 1.2 mV, p=0.73), membrane resistance (CTL 140.0 ± 18 MOhm, MUT 132.5 ± 12 MOhm, p= 0.74) or capacitance (CTL 42.5 ± 3.1 pF, MUT 43.5 ± 3.9 pF, p=0.85) (**Figure 5- figure supplement**

1A). In sum, CNO effectively increases firing in FS CINs and ERK1/2 signaling is not necessary for the development of FS CIN intrinsic excitability.

During the emergence of $GABA_AR$-mediated inhibition ~P7 in the cortex, activity is especially critical for the survival and maturation of CINs (De Marco García et al., 2011; Hanson et al., 2019; Lodato et al., 2011; Okaty et al., 2009; Pan et al., 2018; Southwell et al., 2012). To directly assess the role of chronic changes in activity on CIN development in vivo, we treated *Erk1*$^{-/-}$, *Erk2*$^{fl/wt}$, *Nkx2.1*^{Cre}, G_q*-DREADD-HA* control animals with 2 mg/kg CNO or vehicle daily from P8-P14 and measured the expression of the activity-dependent and relatively AP-1 family transcription factor, FOSB (**Figure 5D**). We identified CINs using the haemagglutinin (HA) tag fused to the G_q receptor. Consistent with past studies, we found that ~5% of CINs in vehicle treated controls exhibited detectable FOSB immunoreactivity, whereas we observed higher levels of basal FOSB expression in surrounding excitatory neurons (**Figure 5E-H)** (Hrvatin et al., 2018; Mardinly et al., 2016). One week of daily CNO treatment in control mice led to a significant, 6.3-fold increase in $FOSB^+/HA^+$ co-labeled CINs ($F_{3,14}$=15.37, post-hoc p<.001) (**Figure 5I-K, magenta arrows**). The density of Cre-recombined, HA^+ CINs in the primary somatosensory cortex was unaltered by seven days of CNO treatment at this age (**Figure 5-figure supplement 1B**).

In excitatory neurons, ERK1/2 signaling is an important regulator of activity-dependent gene expression (Thomas & Huganir, 2004). However, this has not been directly tested in developing CINs, which exhibit notable differences in activity-dependent gene programs (Hrvatin et al., 2018; Mardinly et al., 2016; Sik et al., 1998). To understand the contributions of ERK1/2 signaling to activity-dependent responses in developing CINs *Erk1*$^{-/-}$, *Erk2*$^{fl/fl}$, *Nkx2.1*^{Cre}, G_q*-DREADD-HA* mutant mice were treated with CNO or vehicle from P8-P14. Vehicle-treated,

Erk1/2 mutants did not exhibit significant differences in the proportion of FOSB$^+$/HA$^+$ CINs when compared to vehicle treated controls (**Figure 5E-N**). Importantly, chemogenetic depolarization-induced FOSB expression was significantly reduced in *Erk1/2* mutant CINs treated for seven days with CNO when compared to CNO treated controls (**Figure 5E-Q**) ($F_{3,14}$=15.37, post-hoc p<.001). We found that hyperactivation of MEK-ERK1/2 signaling alone in *Mek1$^{S217/221E}$*, *Nkx2.1^{Cre}*, *Ai9* mice was not sufficient to alter basal FOSB expression in CINs (**Figure 5- figure supplement 1C-E**). Together, these data demonstrate that ERK1/2 signaling is necessary for chemogenetic activity-dependent FOSB expression in CINs.

Chemogenetic stimulation during development increases SST expression in Erk1/2 deleted CINs.

Our results suggest ERK1/2mediates select aspects of activity dependent signaling, however, chronic chemogenetic activation could activate parallel pathways that compensate for the loss of *Erk1/2* during development. We therefore assessed whether one week of daily CNO treatment between P8 and P14 modified the proportion of SST$^+$/HA$^+$ cells in the somatosensory cortex. In control *Erk1$^{-/-}$*, *Erk2$^{fl/wt}$*, *Nkx2.1^{Cre}*, *G_q-DREADD-HA* animals, we found that increasing activity during the second postnatal week did not significantly alter the proportion of SST$^+$/HA$^+$ CINs ($F_{3,14}$ = 22.83, post-hoc p=0.144) (**Figure 6A-F**). However, chemogenetic stimulation of *Erk1$^{-/-}$*, *Erk2$^{fl/fl}$*, *Nkx2.1^{Cre}*, *G_q-DREADD-HA* mutants induced a significant increase in SST$^+$/HA$^+$ CINs relative to vehicle-treated mutants (**Figure 6B, G-J**) ($F_{3,14}$ = 22.83, post-hoc p=0.005). We did not observe co-expression of PV and SST in HA$^+$ neurons, indicating that chemogenetic activation did not induce ectopic SST expression in FS CINs. Together, these data indicate one week of chemogenetic stimulation during early development is sufficient to restore, in part, SST-CIN number following the loss of ERK1/2.

ERK1/2 signaling is required for activity-dependent FOSB expression in adult CINs.

Early cortical circuits may be uniquely capable of responding to altered activity relative to adult stages. We tested the role of ERK1/2 in activity-dependent FOSB expression in adult CINs between 6-10 months of age (**Figure 7A**). Following one week of daily CNO administration to adult *Erk1*$^{-/-}$, *Erk2*$^{fl/wt}$, *Nkx2.1*^{Cre}, G_q*-DREADD-HA* controls, we noted a significant increase in the proportion of CINs expressing FOSB when compared to vehicle treated controls ($F_{3,8}$ = 31.88, post-hoc p<0.001) (**Figure 7B**, **Figure 7- figure supplement 1A-D**). As in young mice, adult CNO-treated *Erk1*$^{-/-}$, *Erk2*$^{fl/fl}$, *Nkx2.1*^{Cre}, G_q*-DREADD-HA* mutant CINs displayed significantly less FOSB induction than CNO-treated controls ($F_{3,8}$ = 31.88, post-hoc p<0.001) (**Figure 7B**, **Figure 7- figure supplement 1A-D**). The overall pattern and number of non-recombined FOSB$^+$ cells across the primary somatosensory cortex were relatively unaffected by CIN-specific ERK1/2 deletion or chronic chemogenetic stimulation (**Figure 7- figure supplement 1E-H, M**). Adult *Erk1*$^{-/-}$, *Erk2*$^{fl/wt}$, *Nkx2.1*^{Cre}, G_q*-DREADD-HA* control animals treated with CNO showed a significant increase in voluntary locomotion compared with vehicle-treated controls as measured by the distance traveled in an open field chamber (**Figure 7C**, **Figure 7- figure supplement 1I-L**) ($F_{3,29}$ = 10.07, post-hoc p=0.001). In contrast, *Erk1*$^{-/-}$, *Erk2*$^{fl/fl}$, *Nkx2.1*^{Cre}, G_q*-DREADD-HA* mutants did not exhibit significantly increased locomotion following CNO administration (**Figure 7C**, **Figure 7- figure supplement 1I-L**) ($F_{3,29}$ = 10.07, post-hoc p=0.553). The *Nkx2.1*^{Cre} derived neurons that might contribute to locomotor activity are widespread across the CNS. These data demonstrate that ERK1/2 is broadly required for chemogenetic activation of mature CINs and possibly other neuronal populations involved in locomotion (Xu et al., 2008).

Finally, we tested whether seven days of chemogenetic stimulation during adulthood altered the proportion of SST-CINs. Following one week of daily CNO treatment, control animals showed no change in the proportion of SST^+/HA^+ cells in the primary somatosensory cortex (**Figure 7D**). In mutant animals, however, we found a modest but statistically significant increase in the proportion of SST^+/HA^+ cells following CNO treatment relative to vehicle treated mutants (**Figure 7D-L**) ($F_{3,12}$ =126.54, post-hoc p=0.024). These data suggest that chemogenetic restoration of SST-CINs in *Erk1/2* mutants can occur well into adulthood.

Discussion

Over the course of development, CINs respond to well-defined extracellular cues that regulate proliferation, specification, and the release of neurotransmitters critical for cortical function. Yet the role of associated downstream intracellular signaling cascades in vivo has received less attention. Here, we show that ERK1/2 activity in MGE derivatives is critical for the establishment of glial number but is not necessary for CIN survival or initial commitment to a GABAergic fate. However, we found that ERK1/2 is important for activity dependent expression of FOSB in CINs and regulates the number of SST-expressing, but not PV-expressing, GABAergic neurons. Interestingly, in vivo chemogenetic stimulation of mutant CINs was sufficient to partially overcome the effect of *Erk1/2* inactivation and increase the proportion of CINs expressing SST. These data provide new insight into the specific signaling requirements of developing MGE-derivatives and the cellular functions of ERK1/2 in the development of cortical inhibitory circuits.

Our findings show that loss of ERK1/2 significantly decreases glial number in the anterior commissure, while hyperactive MEK-ERK1/2 signaling is sufficient to increase MGE-derived oligodendrocyte number. These results are consistent with previous findings in neural progenitor domains in the dorsal cortex and peripheral nervous system (Dinh Duong et al., 2019; Filges et al., 2014; X. Li et al., 2012; Newbern et al., 2011). Upstream RASopathy mutations in *Ras* and *NF1* alter multiple parallel kinase cascades, including ERK1/2, and increase glial number (Angara et al., 2020; Breunig et al., 2015; Gutmann et al., 2001; Holter et al., 2019; Krencik et al., 2015; Rizvi et al., 1999). Our data further indicate a critical requirement for ERK1/2 signaling in establishing myelinating glial number across the nervous system, despite substantial differences in origin and local extracellular environments. Whether reduced *ERK1/MAPK3*,

ERK2/MAPK1, or *MEK2/MAP2K2* gene dosage in individuals with 16p11.2-, distal22q11.2-, or 19p13.3-microdeletions, respectively, is sufficient to disrupt myelinating glial number and contribute to abnormal white matter microstructure in some of these conditions is unclear (Qureshi et al., 2014). This conserved functional link may also be an important consideration in pediatric RASopathy clinical trials utilizing prolonged pharmacological ERK1/2 pathway inhibition.

Past studies have shown that distinct neuronal populations arising from the same progenitor domain exhibit unexpectedly diverse cellular responses to ERK1/2 modulation (Holter et al., 2021; Hutton et al., 2017; Newbern et al., 2011; Sanchez-Ortiz et al., 2014; Vithayathil et al., 2015; L. Xing et al., 2016). In many non-neuronal cells, ERK1/2 and PI3K/AKT are important regulators of proliferation, migration, and survival (Lavoie et al., 2020). In CINs, PI3K/AKT mediates comparable cellular behaviors (Oishi et al., 2009; Polleux et al., 2002; Vogt et al., 2015; Wei et al., 2020; Wong et al., 2018). In contrast, we found that ERK1/2 is not necessary for CIN migration or survival. This outcome differs from the previously reported requirement for ERK1/2 signaling in excitatory corticospinal neuron survival during the neonatal period (L. Xing et al., 2016). The mouse models we have generated will provide important tools for further dissection of the precise mechanisms that regulate these context-dependent functions.

Early CIN development is determined, in part, by local morphogen gradients acting via specific transcriptional programs (Hu et al., 2017; Lim et al., 2018). For example, SHH signaling is required for the specification of MGE-derived GABAergic neurons during mid embryogenesis and later biases these neurons toward a SST fate (Tucker et al., 2008; Tyson et al., 2015; Xu et al., 2005, 2010; Yu et al., 2009). In certain contexts, ERK1/2 signaling has been shown to non-canonically activate GLI1, a well-known transcriptional target of SHH (Pietrobono et al., 2019;

Po et al., 2017). It is possible that SHH and ERK1/2 signaling converge on GLI1 to direct neurons toward a SST-CIN fate. Future studies will be necessary to identify the molecular mediators that activate ERK1/2 and regulate the proportion of SST-CINs in the developing CNS.

Cortical circuit formation establishes a complex balance between GABAergic and glutamatergic signaling. GABA-mediated signals promote the maturation of excitatory neurons, in part via ERK1/2 dependent mechanisms (Cancedda et al., 2007; Obrietan et al., 2002; Peerboom & Wierenga, 2021). Past reports demonstrate that early alterations in CIN number or activity can permanently change circuit architecture and animal behavior (Bitzenhofer et al., 2021; Kaneko et al., 2022; Magno et al., 2021; Tuncdemir et al., 2016). Here, we employed a chemogenetic approach to selectively activate CINs with temporal specificity. We found that CIN-targeted chemogenetic stimulation during the second postnatal week did not alter CIN number. Past studies have identified a role for activity in early CIN survival (Denaxa et al., 2018; Priya et al., 2018; Southwell et al., 2012; Wong et al., 2018). However, we modulated the activity of endogenous CINs at a stage past the peak of CIN apoptosis and after $GABA_A$Rs acquire inhibitory responses (Ben-Ari et al., 2007, p.; Denaxa et al., 2018; Southwell et al., 2012; Wong et al., 2018). We did note that activation of *Nkx2.1*-derived cells in adults alters locomotor behavior in an ERK1/2-dependent manner. It is unclear which neuronal subtypes mediate this effect, as *Nkx2.1*^{Cre} lineages populate many areas, including the striatum and ventral forebrain that influence motor behavior (Fu et al., 2014; Hutton et al., 2017; Xu et al., 2008). In future studies, it will be important to investigate how ERK1/2 signaling in CINs influences more complex behaviors (Adler et al., 2019; Chen et al., 2019; Cummings & Clem, 2020; Fu et al., 2014; Kluge et al., 2008; C. Lee et al., 2022; Magno et al., 2021).

Recent work has led to a deeper appreciation for the unique contributions of CIN subtypes to cortical microcircuits. Here, we found that ERK1/2 is critical for SST protein expression in a subset of CINs, without a change in total CIN number. SST mRNA is first detected in immature CINs by mid-embryogenesis, but substantial levels of SST protein are not observed in CINs until early neonatal stages (Batista-Brito et al., 2008; Denaxa et al., 2012; Forloni et al., 1990; D. R. Lee et al., 2022; Neves et al., 2013; Taniguchi et al., 2011). A loss of SST protein has been seen in a number of other neuropathological conditions, but has not been directly assessed in conditions characterized by reduced ERK1/2 signaling (Davies et al., 1980; Fee et al., 2017; Pantazopoulos et al., 2017; Peng et al., 2013; Robbins et al., 1991; Sun et al., 2020; Tripp et al., 2011; Wengert et al., 2021). SST is not only a marker of RS-CINs, but an active neuropeptide with biological functions (Baraban & Tallent, 2004; Grilli et al., 2004; Liguz-Lecznar et al., 2016; Smith et al., 2019; Song et al., 2021; Tereshko et al., 2021). The release of bioactive neuropeptides from subtypes of CINs likely contributes to cortical computation (Ouwenga et al., 2018; Smith et al., 2019). Indeed, a recent report demonstrated that SST infusion into V1 can improve performance in a visual discrimination task, independent of GABA (Song et al., 2020). Administration of SST or synthetic analogues may compensate for the aberrant development of SST-CINs in ERK1/2 loss of function models (Banks et al., 1990; Engin & Treit, 2009; Kiviniemi et al., 2015; McKeage, 2015). Approaches that target SST may have broader applications in the treatment of neurodevelopmental disorders, particularly cases of epilepsy, autism, and schizophrenia where deficits in SST-CIN function are well described (Song et al., 2021).

Interestingly, one week of chemogenetic stimulation partially restored SST expression in *Erk1/2*-deleted CINs at both juvenile and adult stages. Chemogenetic depolarization may engage

several parallel cascades including cAMP/PKA, Ca^{2+}, PKC, and ERK1/2, which have been shown to activate and often converge on common transcriptional targets, such as CREB, SRF, and AP-1 family members (Yap & Greenberg, 2018). We demonstrated that the activity-dependent expression of FOSB, a CREB target, requires ERK1/2, similar to glutamatergic neurons (Guenthner et al., 2013; Hrvatin et al., 2018; Mardinly et al., 2016; Spiegel et al., 2014). Interestingly, one of the first CREB target genes to be identified was SST (Montminy & Bilezikjian, 1987; Yamamoto et al., 1988). Chemogenetic activation of ERK1/2-independent cascades may be sufficient to partially compensate for the loss of *Erk1/2* and modestly restore SST expression in CINs. Whether other activity-dependent genes critical for CIN plasticity are similarly restored remains to be seen. Our finding that adult chemogenetic activation partially restored SST expression raises the possibility that late-stage therapeutic interventions may improve aspects of CIN function in ERK1/2-related syndromes.

Acknowledgements:

We thank Chris Wedwick, Anna Bayne, and Elise Bouchal for technical assistance with mouse sample processing and image analysis. This research is supported by the National Institute of Health grants R00NS076661 and R01NS097537 awarded to JMN. SK is supported by the ARCS Foundation. AMS and DV are supported by the Spectrum Health-Michigan State Alliance Corporation, Autism Research Institute pilot grant and Department of Defense grant NF200109. TA and GL are supported by the University of Arizona – COM Phoenix "Springboard" award. We deeply appreciate the support of the ASU Keck Bioimaging facility and ASU Personalized Diagnostic Core for outstanding technical advice and support.

Conflict of Interest Statement

The authors declare no competing interests.

Materials and Methods

Genetically modified mice

All mice were handled and housed in accordance with the guidelines of the Institutional Animal Care and Use Committee at Arizona State University or Michigan State University. Mice were fed *ad libitum* and were housed under a 12-hour light-dark cycle. All mature mice examined in this study were euthanized via CO2 inhalation or IACUC-approved chemical anesthetics prior to transcardial perfusion, while embryonic/neonatal mice were cryoanesthetized, as described in the AVMA Guidelines on Euthanasia. The following strains of mice were utilized in this work.

Mouse Strains	Details	Reference	Identifier
Erk1/Mapk3$^{-/-}$	Neo cassette inserted into Exon 1-6 of *Erk1/Mapk3*	(Selcher, 2001)	RRID:IMSR_JAX :019113
Erk2/Mapk1$^{loxp/loxp}$	Exon 2 in *Erk2/Mapk1* flanked by loxp sites	(Samuels et al., 2008)	RRID:IMSR_JAX :019112
CAG-LSL-Mek1$^{S217/221E}$	Cre-dependent hyperactive Mek1 overexpressing mice	(Krenz et al., 2008)	MGI:3822131
Nkx2.1^{Cre}	Cre recombinase expression in radial glia in the MGE, POA, and other regions by E8.5	(Xu et al., 2008)	RRID:IMSR_JAX :008661
Slc32a1/VGAT^{iresCre}	Cre recombinase expression in all postmitotic GABAergic neurons, including CINs by E11.5	(Vong et al., 2011)	RRID:IMSR_JAX :016962
Dlx5/6^{Cre}	Cre recombinase expression in a subset of postmitotic cortical GABAergic neurons and other regions by E9.5	(Monory et al., 2006)	RRID:IMSR_JAX :008199
LSL-Gq-DREADD	Cre-dependent HA-hM3Dq-pta-mCitrine expressing line	(Zhu et al., 2016)	RRID:IMSR_JAX :026220
LSL-Rpl22^{HA}	Cre-dependent RNA immunoprecipitation line	(Sanz et al., 2009)	RRID:IMSR_JAX :011029

Ai3 / Ai9 / Ai14	Cre-dependent fluorescent protein (EYFP or tdTomato) expressing lines	(Madisen et al., 2010)	RRID:IMSR_JAX :007903, 007908, 007903

To generate *Erk1/Erk2* loss-of-function mutants, mice expressing *Nkx2.1*^{Cre}, *Slc32A1/VGAT*^{Cre}, or *Dlx5/6*^{Cre} were bred with mice possessing a neo-insertion in exons 1-6 in the *Erk1/Mapk3* gene (referred to as *Erk1*$^{-}$) and/or a loxp-flanked exon 2 in the *Erk2/Mapk1* gene (referred to as *Erk2*^{fl}) (Monory et al., 2006; Samuels et al., 2008; Selcher, 2001; Xu et al., 2008). Littermates expressing Cre recombinase and heterozygous *Erk2*$^{fl/wt}$ were used as controls for loss-of-function experiments unless indicated otherwise. Cre-dependent tdTomato/RFP (*Ai9 or Ai14*) or eYFP (*Ai3*) strains were employed to fluorescently-label Cre-expressing cells (Madisen et al., 2010).

Conditionally hyperactive MEK-ERK1/2 mutants were generated by crossing *Nkx2.1:Cre* mice with *CAG-lox-STOP-lox-Mek1*$^{S217/221E}$ (referred to as *Mek1*$^{S217/221E}$) mice on a mixed genetic background to generate double heterozygous mutants expressing *Mek1*$^{S217/221E}$ in a Cre-dependent pattern. *Mek1*$^{S217/221E}$ mice were kindly provided by Dr. Maike Krenz and Dr. Jeffrey Robbins (Krenz et al., 2008).

For chemogenetic experiments, an *loxp-STOP-loxp-*G_q*-DREADD-HA* line was used, which produces the engineered G-protein coupled receptor, hM3D$_q$, with a hemagglutinin (HA) tag in Cre-expressing cells (Zhu et al., 2016). To chemogenetically stimulate neurons in vivo, mice of the indicated age received an intraperitoneal injection of 2 mg/kg body weight clozapine-*N*-oxide (CNO) or 0.09% NaCl saline vehicle every 24 hours for 7 consecutive days. Body weight and time of injection were recorded each day and tissue was collected 2 hours after the last dose of CNO.

PCR Genotyping

Genomic DNA was rapidly extracted from mouse tissue samples for PCR genotyping with 25mM NaOH, 0.2 mM EDTA, pH=12 and subsequently neutralized with 40 mM Tris-Cl, pH=5. The primers used for genotyping were as follows: (listed 5'-3'): *Cre* – TTCGCAAGAACCTGATGGAC and CATTGCTGTCACTTGGTCGT to amplify a 266 bp fragment; *Erk1*$^{-}$ – AAGGTTAACATCCGGTCCAGCA, AAGCAAGGCTAAGCCGTACC, and CATGCTCCAGACTGCCTTGG to amplify a 571 bp segment wild type and a 250 bp segment KO allele; *Erk2*^{fl} – AGCCAACAATCCCAAACCTG, and GGCTGCAACCATCTCACAAT amplify 275 bp wild-type and 350 bp floxed alleles; *Ai3/Ai9* – four primers were used - AAGGGAGCTGCAGTGGAGTA, CCGAAAATCTGTGGGAAGTC, ACATGGTCCTGCTGGAGTTC, and GGCATTAAAGCAGCGTATCC amplify a 297 bp wt Rosa26 segment and a 212 bp *Ai3*/*Ai9* allele; *hM3Dq* – CGCCACCATGTACCCATAC and GTGGTACCGTCTGGAGAGGA amplify a 204 bp fragment; *Mek1*$^{S217/221E}$ – GTACCAGCTCGGCGGAGACCAA and TTGATCACAGCAATGCTAACTTTC amplify a 600 bp fragment.

Tissue Preparation and Immunostaining

Mice of the specified age were fully anesthetized and perfused with cold 1X PBS followed by 4% PFA in a 1X PBS solution. Brains were then removed and post-fixed at 4C. Brains were sliced with a vibratome or were cryoprotected for preparation on a cryostat. Sectioned brain tissue was then incubated for 24-48 hours at 4ºC in a primary antibody solution diluted in .05 – 0.2% Triton in 1X PBS with 5% Normal Donkey Serum (NDS). Primary antibody information is provided in the table below.

Antibody	Host & Usage Details	Source	Identifier
Anti-Somatostatin	Rabbit, 1:1000	Peninsula/BMA Biomed.	(Peninsula Laboratories Cat# T-4103.0050, RRID:AB_518614)
Anti-Somatostatin	Guinea Pig, 1:1000	Synaptic Systems	(Synaptic Systems Cat# 366 004, RRID:AB_2620126)
Anti-Parvalbumin	Goat, 1:1000	SWANT	(Swant Cat# PVG-213, RRID:AB_2650496)
Anti-GFP	Chicken, 1:1000	Aves	(Aves Labs Cat# GFP-1020, RRID:AB_10000240)
Anti-RFP	Chicken, 1:1000-1:2000	Rockland	(Rockland Cat# 600-901-379, RRID:AB_10704808)
Anti-RFP	Rabbit, 1:1000	Rockland	(Rockland Cat# 600-401-379, RRID:AB_2209751)
Anti-ERK2	Rabbit	Abcam	(Abcam Cat# ab32081, RRID:AB_732210)
Anti-Calbindin 1	Chicken, 1:1000	Novus	NBP2-50028
Anti-NeuN	Mouse, 1:1000	Millipore	(Millipore Cat# MAB377, RRID:AB_2298772)
Anti-HA	Mouse, 1:1000	Biolegend	(BioLegend Cat# 901513, RRID:AB_2565335)
Anti-FOSB	Rabbit, 1:1000	Abcam	(Abcam Cat# ab184938, RRID:AB_2721123)
Anti-MEK1	Rabbit, 1:1000	Abcam	(Abcam Cat# ab32091, RRID:AB_776273)
Anti-GFAP	Rabbit, 1:1000	Abcam	(Abcam Cat# ab7260, RRID:AB_305808)
Anti-OLIG2	Rabbit, 1:1000	Millipore	(Millipore Cat# AB9610, RRID:AB_570666)

Sections were then washed three times in 1X PBS .05% Triton and incubated in a solution containing secondary antibodies diluted to 1:1000 in 1X PBS .05 – 0.2% Triton and 5% NDS. A Zeiss LSM710 or LSM800 laser scanning confocal microscope was used to collect images.

Representative confocal images were optimized for brightness and contrast in Adobe Photoshop and compiled into figures with Adobe Illustrator.

Image Analysis

Images from a minimum of three mice per genotype were collected and multiple sections containing the anatomical region of interest were quantified per mouse by an observer blinded to the conditions. To estimate labeled cell density, region of interests were defined using standard anatomical and architectonic landmarks, the area was measured in Photoshop, and labeled cells were quantified. Cortical density measurements are derived from counts collected across an entire cortical column. For comparisons involving two groups, data were statistically analyzed with an unpaired, two-tailed t-test. For comparisons involving four groups, a one-way ANOVA and Fisher's LSD post-hoc tests were performed in IBM SPSS Statistics 28.

RNA collection and sequencing

RNA collection and ribosome immunoprecipitation from brain samples was performed essentially as described in Sanz et al., 2009. Whole P7.5 cortices were rapidly dissected, rinsed, and Dounce homogenized in 500 µL of ice-cold RNase-free buffer polysome buffer (50 mM Tris pH 7.5, 100 mM KCl, 12 mM MgCl2, 1% NP-40, 1 mM DTT, 200U/ml Promega RNasin, 1 mg/ml heparin, 100 µg/ml cycloheximide, and protease inhibitors). The lysate was cleared via centrifugation at 10,000g for 20 min at 4ºC. 60 µl of supernatant ("INPUT") containing RNA derived from the entire cortical sample was collected and lysed with 350 µl of buffer RLT from Qiagen RNeasy Kit supplemented with 10µl/ml bME. Rpl22^{HA}-containing ribosomes were immunoprecipitated ("IP") from the remaining supernatant by gently mixing with 5µl of rabbit

anti-HA antibody (#71–5500 Thermo Fisher Sci) and incubating with gentle rocking at 4°C for 2 hours before isolation with 50 µl of protein A/G magnetic beads previously equilibrated in polysome buffer and a magnetic stand. Immunoprecipitates were rinsed 3x with 800 µl of a high salt buffer (50 mM Tris pH 7.5, 300 mM KCl, 12 mM MgCl2, 1% NP-40, 1 mM DTT, 100 µg/ml cycloheximide) and then lysed in 350 µl of buffer RLT. RNA isolation from INPUT and IP fractions was performed following manufacturer's instructions using Qiagen's RNeasy extraction kit with DNAse digestion. RNA quantitation was performed using a Ribogreen RNA reagent and samples with an RNA integrity number < 7 on an Agilent Bioanalyzer were selected for sequencing.

2 ng of purified RNA were used for single primer isothermal amplification (SPIA) and generation of double-stranded cDNA with the Ovation RNAseq System V2 per manufacturer instructions (Nugen Technologies). Library construction and sequencing were performed on the Illumina NextSeq 500 platform at the Arizona State University's Genomics Core facility. RNAseq reads were quality checked, filtered, aligned to the mouse genome Ensembl GRCm38 primary assembly using RNA-STAR, and read counts were estimated using featureCounts (Dobin et al., 2013). DEXseq was employed to measure differential exon usage in *Erk1* exons 1-6 and *Erk2* exon 2 (Anders et al., 2012). Analysis with DeSeq2 resulted in >11,000 protein-coding genes in each sample with a normalized count > 50 (**Table S1**) (Love et al., 2014). Protein-coding genes were considered differentially expressed if the CoV of normalized DeSeq2 counts within a condition were < 90 and the fold-change between conditions was >1.5 with an unadjusted p-value <.05 (**Table S2**). Raw sequencing data are available in NCBI's Gene Expression Omnibus repository at accession number GSE206633 (Edgar et al., 2002).

Electrophysiology

For electrophysiological experiments, postnatal day 15-22 (P15-22) mice were used for the preparation of in vitro whole-cell patch-clamp experiments as previously reported (Anderson et al., 2010; Goddeyne et al., 2015; Holter et al., 2021; Nichols et al., 2018). The somatosensory cortices of these mice were injected with a Cre-dependent AAV9-FLEX-tdTomato (Addgene catalog #28306-AAV9) viral vector solution between P0-P2 to unambiguously label a subset of recombined CINs for fluorescently-guided patch clamping. In brief, mice were then deeply anesthetized by isoflurane inhalation before decapitation. Brains were quickly removed and immersed in the saturated (95% O_2, 5% CO_2), ice-cold artificial cerebral spinal fluid (aCSF), which contains (in mM): 126 NaCl, 26 $NaHCO_3$, 2.5 KCl, 10 Glucose, 1.25 $Na_2H_2PO_4H_2O$, 1 $MgSO_4{\cdot}7H_2O$, 2 $CaCl_2H_2O$, pH 7.4. Coronal slices from the region of the somatosensory cortex (350 μm in thickness) were collected with a vibratome (VT 1200; Leica, Nussloch, Germany). Following the preparation of brain slices, they were allowed to recover in the same aCSF at 32ºC for 30 minutes before being moved to room temperature for an additional 30 minutes. For patch-clamp recordings, slices were transferred into a submerged recording chamber and perfused continuously with aCSF at 32ºC at a rate of 1-2 ml/min. Whole-cell patch-clamp recordings were obtained from fluorescent positive neurons in layer V (L5) of the somatosensory cortex by using an Axon 700B amplifier. The data were filtered at 2 kHz and sampled at 10 kHz via a digitizer (Digidata 1440, Molecular Devices) and recorded using Clampex 10.6 software (Molecular Devices). The pipettes had a resistance of 2-5 MΩ when filled with the internal solution which contains (in mM): 135 K-Gluconate, 4 KCl, 2 NaCl, 10 HEPES, 4 EGTA, 4 Mg ATP and 0.3 Na Tris. Pipettes were pulled from borosilicate glass (BF150-110-10, Sutter Instruments) by using a Sutter Instrument puller (Model P-1000). The stability of the recordings was monitored

throughout the experiment and recordings with series resistances (Rs) larger than 25 MΩ or a change of more than 20% were abandoned.

Data were analyzed using Clampfit software (Molecular Devices) and results were presented as mean ± SEM. Membrane resistance (Rm) and capacitance (Cm) were calculated from the response to a voltage step (5mV). Resting membrane potential was measured during current-clamp recording prior to the introduction of steps (-200pA, 0 or 200pA, 1 s duration) used in examining the firing properties of the neurons. For calculation of CNO induced changes in holding current, neurons were recorded under voltage clamp at -70mV. The change in holding current was calculated by subtracting the baseline value (i.e., in aCSF) from that measured after 20 minutes of bath application of CNO (10 µM). At this time point, CNO-induced changes in holding current had reached a steady-state plateau. Data were compiled and appropriate statistical analysis was performed using Prism software (Graphpad) and figures compiled in CorelDraw (Corel Corporation) and Adobe Illustrator. For all electrophysiological statistics, $p < .05$ was considered statistically significant and tested with an unpaired student t-test unless otherwise indicated.

Open Field

The open field test was used to measure voluntary locomotor capabilities in mice on the second day of CNO or vehicle treatment, two hours after CNO injection. The open field apparatus consisted of a 40 × 40 cm Plexiglas arena enclosed by 30-cm-high opaque walls. A single 60W bulb was positioned to brightly illuminate the center of the chamber with dim lighting near the walls. Mice were placed into the center of the apparatus and video recorded for a total of 5 min. Video data were analyzed for total distance traveled.

634

Figure Legends

Figure 1. ERK1/2 signaling regulates MGE-derived oligodendrocyte number. (A) Low magnification image of a P14 control *Nkx2.1*^{Cre}, *Ai9*$^{+/-}$ coronal section showing the expected neuroanatomical pattern of RFP^{+} cells. **(B-G)** Representative confocal images of the anterior commissure at P14 display a significant decrease in the density of OLIG2^{+}/RFP^{+} co-labeled cells in *Erk1*$^{-/-}$, *Erk2*$^{fl/fl}$, *Nkx2.1*^{Cre}, *Ai9* mutants compared to controls (quantification in **H**; N=3, mean ± SEM, *student's t-test, *p*=.0002) (scale bars 100µm (B-C), 50µm (D-G)). **(I-L)** Confocal images of the anterior commissure at P21 revealed a significant increase in the number of OLIG2^{+}/RFP^{+} cells in *Mek1*$^{S217/221E}$, *Nkx2.1*^{Cre}, *Ai9* mutants relative to controls (scale bar = 50 µm) (Quantification in **M**; N=3-4, mean ± SEM, *student's t-test, *p*=.004). **(N-Q)** We observed ectopic expression of OLIG2^{+}/RFP^{+} cells in the fimbria of *Mek1*$^{S217/221E}$, *Nkx2.1*^{Cre}, *Ai9* mutants (scale bar = 50 µm) (quantification in **R**; N=3-4, mean ± SEM, *student's t-test, *p*=.005).

Figure 1-figure supplement 1: Cre-targeted modulation of ERK1/2 signaling. (A) Coronal section of an E13.5 *Nkx2.1*^{Cre}, *Ai9* brain showing the pattern of Cre-mediated recombination. **(B)** Summary of cell counts of *Nkx2.1*-derived cells in the anterior commissure at P14 and P21. **(C-N)** High-resolution confocal images of neurons (C-H) and glia (I-N) demonstrating reduced ERK2 immunoreactivity in RFP-expressing cells in P14 *Erk1*$^{-/-}$, *Erk2*$^{fl/fl}$, *Nkx2.1*^{Cre}, *Ai9* mice (scale bar = 5µm). **(O-Z)** High-resolution confocal images demonstrating an increase in MEK1 expression in both RFP^{+} neurons (O-T) and glia (U-V) in *Mek1*$^{S217/221E}$; *Nkx2.1*^{Cre}, *Ai9* animals (scale bar = 5µm).

Figure 2: ERK1/2 deletion does not alter CIN number. (A-E) Representative images of P14 somatosensory cortex in control (A-B) and *Erk1*$^{-/-}$, *Erk2*$^{fl/fl}$, *Nkx2.1*^{Cre}, *Ai9* (C-D) animals, showing similar density of Cre^{+} cells (quantification in **E**, N=4, mean +/- SEM, student's t-test, p=0.476**)** (scale bar = 50µm) **(F-J)** At P5, control (F-G) and *Erk1*$^{-/-}$, *Erk2*$^{fl/fl}$, *VGAT*^{Cre}, *Ai9* animals (H-I) showed no significant difference in the density of RFP^{+} cells in the somatosensory cortex (quantification in **J**, N=4, mean +/- SEM, student's t-test p=.955) (scale bar = 50µm).

Figure 2-figure supplement 1. Cre-mediated deletion of ERK1/2 does not alter CIN number. (A) Coronal section of P6 *Erk1*$^{-/-}$, *Erk2*$^{fl/fl}$, *VGAT*^{Cre}, *Ai9* brain demonstrating the pattern of Cre-mediated recombination. **(B-G)** Confocal images confirming ERK2 reduction in CINs (scale bar = 5µm). **(H-K)** Representative images of P14 somatosensory cortices showing comparable density of *Ai3*$^{+}$ cells in *Erk1*$^{-/-}$, *Erk2*$^{fl/wt}$, *Dlx5/6*^{Cre}, *Ai3* controls and *Erk1*$^{-/-}$, *Erk2*$^{fl/fl}$, *Dlx5/6*^{Cre}, *Ai3* mutants.

Figure 3. Loss of ERK1/2 does not alter the initial specification of generic regulators of GABAergic function. **(A)** HET IP vs MUTANT IP volcano plot of expressed protein-coding genes in CIN-enriched samples illustrates the significant reduction in ERK1/2 pathway target genes in *Erk1/2* inactivated CINs (magenta - *Spry4, Etv5, Egr2*) (N=3, p<.05). A significant difference was not detected in the expression of master regulators of CIN specification (green - *Lhx6, Dlx2/5/6*) and key GABA processing genes (green - *Gad1/2, Slc32a1*). However, the expression CIN-subtype enriched genes (*Crhbp, Sst, Mafb, Grin2d, Sp9*) and canonical developmental signals (*Notch1, Smo, Fgf18, Bdnf*) were significantly altered in mutant CINs. **(B-J)** Immunolabeling analysis of CIN subtype markers revealed a significant reduction in

$SST^+/CALB^-$ cell density (yellow arrowheads) in mutants, while $SST^+/CALB^+$ co-labeled cell density was unchanged (quantification in **B**, N=4, mean ± SEM, *student's t-test p=0.017). Representative images in (D-J) are from layer 5 primary somatosensory cortex (scale bar = 25µm).

Figure 3-figure supplement 1. RiboTag in ERK VGAT mouse enriches for GABAergic interneurons. (A) Read coverage maps for *Erk1/Mapk3* and *Erk2/Mapk1* in a representative immunoprecipitated RNA sample from a wildtype, heterozygous control, and mutant *Erk1 Erk2 VGAT^{Cre} Rpl22^{HA}* cortex. *Erk1* exons 1-6 were not detected in heterozygous (N=3) and mutant (N=3) fractions relative to wildtype (N=2) samples (DEXSeq: p<0.005). Analysis of *Erk2/Mapk1* exon 2 (inset), which is *loxp*-flanked in conditional knockouts, revealed a statistically significant reduction in immunoprecipitated mutant samples when compared to heterozygote controls (DEXSeq: 2.5-fold-reduction, p<0.005, N=3). **(B)** Heatmap of DeSeq2-derived normalized gene expression values for select protein coding genes with known specificity for CINs, excitatory neurons, pan-glia, astrocytes, and oligodendrocytes in all samples. Values were unit-variance scaled for each gene within a row for visualization purposes; purple values indicate relative enrichment while green values indicate relative depletion. **(C)** Volcano plots including >11,000 expressed protein coding genes in IP vs INPUT fractions within each of the three test conditions. Grey dots indicate genes not significantly changed, yellow-green dots are significantly enriched genes in INPUT fractions, while blue dots are significantly enriched genes in IP fractions. Select genes known to be expressed in distinct cell types noted in (B) are highlighted.

Figure 4. SST-CINs are selectively vulnerable to reduced ERK1/2 signaling. (A-H) Representative confocal images of the P60 somatosensory cortex in *Erk1/2* mutant mice. At P14, the proportion of PV-expressing CINs was similar between genotypes (**C, G**, quantification in **Q**; N=3, mean ± SEM, student's t-test, $p > .05$), while the proportion of $SST^+/EYFP^+$ cells was significantly lower in mutants compared to controls (**D, H**, quantification in **Q**; N=3, mean ± SEM, *student's t-test, $p = .005$). **(I-P)** By P60, no difference in PV-CINs was detected (**K, O**, quantification in **Q**; N=3, mean ± SEM, $p > .05$), whereas a significant decrease in the density of $SST^+/EYFP^+$ cells in mutant cortices was still apparent (**L, P**, quantification in **Q**; N=3, mean ± SEM, *student's t-test $p = .03$). **(R)** Quantification of Cre-expressing PV-CIN soma size at P14 did not detect a significant difference between mutants and controls (n=105 control, 108 mutant, mean ± SEM, student's t-test, $p > .05$).

Figure 4-figure supplement 1: Complete loss of ERK1/2 signaling is required to alter SST development. (**A-E**) Representative images showing CIN subtypes in the P30 primary somatosensory cortex. *Nkx2.1*^{Cre} mediated deletion of *Erk2* did not alter total Cre-expressing CIN number or SST-CIN density (quantification in **E**, N=3, mean +/- SEM, students t-test $p > .05$) (scale bar = 50 µm). **(F-J)** Hyperactivation of ERK1/2 in *Mek1*$^{S217/221E}$, *Nkx2.1*^{Cre} mice reduced total Cre-expressing CIN density (data not shown) but did not alter SST-CIN density (quantification in **J**; N=3, mean +/- SEM, students t-test $p > .05$) (scale bar = 50 µm).

Figure 5. ERK1/2 is required to induce FOSB expression in CINs after h3MDq-DREADD mediated depolarization. (**A**) Acute treatment of CINs with 10µM CNO led to a depolarizing increase in the holding current in both control and mutant neurons (n=8 neurons/genotype, mean

+/- SEM, paired t-test, p <.05). **(B)** Control and mutant neurons were recorded under current clamp and the response to a depolarizing current step (200pA, 1s) measured. CNO significantly increased the firing frequency induced by the applied current step in both control and mutant neurons when compared to baseline (VEH) (n= 8 neurons/genotype, mean +/- SEM, paired t-test, p<.05). **(C)** Representative traces of firing response to depolarizing current steps from control or mutant neurons indicate that recorded neurons had a primarily fast-spiking electrophysiological phenotype. **(D)** Diagram of the in vivo experimental design. Animals were treated with 2 mg/kg CNO or saline vehicle by IP injection for 7 days beginning at P8. **(E)** One week of chemogenetic stimulation increased FOSB expression in control CINs but not in mutants (mean +/- SEM, N=4-5, one-way ANOVA followed by Fisher's LSD, $F_{3,14}$=15.37, *post-hoc p<.001). **(F-Q)** Representative confocal images of FOSB/HA/PV co-expression in layer 5 somatosensory cortex at P14. White arrowheads indicate HA^+ cells; magenta arrows indicate $FOSB^+/HA^+$ co-labeled cells (scale bar = 25 µm).

Figure 5-figure supplement 1. Intrinsic excitability of CINs is not changed following ERK1/2 modulation. (A) Key CIN intrinsic properties appear to be unaffected by ERK1/2 deletion, as there was no difference in resting membrane potential (p=0.73), membrane resistance (p= 0.74), or capacitance (p=0.85) (n=8 neurons/genotype, student's t-test**)**. **(B)** HA^+ cell density was unchanged by 7 days of CNO treatment (N=4-5, one-way ANOVA, $F_{3,24}$=0.62, p>.05). **(C-E)** Confocal images showing low expression of FOSB in P21 wild-type CINs under basal conditions (C). FOSB expression was relatively unchanged in *Mek1*$^{S217/221E}$, *Nkx2.1*^{Cre} cortices (D) (Quantification in **E**, mean +/- SEM, N=3, student's t-test, p>.05) (scale bar = 25 µm).

Figure 6. Juvenile chemogenetic stimulation increases SST expression in CINs. (A) Low magnification image showing the P14 somatosensory cortex (scale bar = 200 µm). **(B-J)** (C, E, G, I) Representative confocal images of CIN subtypes in P14 somatosensory cortex, layer 5. (D, F, H, J) Monochrome image highlighting somatostatin immunoreactivity in those cells. CNO treatment increased the proportion of CINs expressing SST in ERK1/2 inactivated mutants, though this proportion was significantly lower than in control animals (scale bar = 50µm) (quantification in **B**, N=4-5, one-way ANOVA followed by Fisher's LSD, $F_{3,14}$=22.83, *post-hoc p=.005).

Figure 7. One week of CNO treatment in adulthood induces a partial rescue of SST expression. (A) Animals aged 6-10 months were administered 2 mg/kg CNO or saline vehicle via daily IP injection for one week. The Open Field task was performed on the second day of treatment, two hours after injection. **(B)** One week of CNO treatment increased FOSB expression in control CINs but not *Erk1*$^{-/-}$, *Erk2*$^{fl/fl}$, *Nkx2.1*^{Cre}, G_q*-DREADD-HA* mutant CINs (N=3, one-way ANOVA followed by Fisher's LSD, $F_{3,8}$ =31.87, *post-hoc p<.001). **(C)** CNO treatment increased the distance traveled during the Open Field task in control animals but not *Erk1*$^{-/-}$, *Erk2*$^{fl/fl}$, *Nkx2.1*^{Cre}, G_q*-DREADD-HA* mutants (N=7-9, one-way ANOVA followed by Fisher's LSD, $F_{3,29}$ = 10.07, *post-hoc p<.001). **(D-L)** The proportion of CINs expressing SST is lower in mutants compared to controls. One week of CNO treatment in adulthood modestly increased SST-CINs (quantification in **D**; N=4, one-way ANOVA followed by Fisher's LSD, $F_{3,12}$ =126.54, *post-hoc p=.024). **(E-L)** Confocal images showing immunolabeling for HA, PV, and SST in control and *Erk1*$^{-/-}$, *Erk2*$^{fl/fl}$, *Nkx2.1*^{Cre}, G_q*-DREADD-HA* mutant mice. Yellow

arrowheads indicate SST^+/HA^+ co-labeled cells in layers 4-5 of the primary somatosensory cortex (scale bar =25µm).

Figure 7-figure supplement 1. ERK1/2 is required for activity-dependent responses in adults. (A-D) High magnification images from layer 5 of the adult somatosensory cortex showing FOSB expression within CINs following 7 days of daily CNO treatment. (scale bar = 10µm). **(E-H)** Confocal images of the adult somatosensory cortex layers 2-5, showing the distribution of FOSB+ cells. The density of FOSB+, HA- cells was unchanged in response to ERK1/2 deletion or chemogenetic stimulation (Quantification in **M**, N=3, one-way ANOVA, $F_{3,8} = 0.16$, $p>.05$) (scale bar = 100µm). **(I-L)** Representative traces of animal movement during the entirety of the 5-minute open field task.

Table S1. Normalized counts and enrichment of expressed protein-coding genes. Protein-coding gene expression in immunoprecipitated (IP) and whole cortical input (INPUT) fractions from all genotypes. DeSeq2 was used to identify differentially expressed genes between IP and INPUT samples within a genotype and calculate average vst-normalized read counts, log2 fold-change, and *p*-value.

Table S2. Differentially expressed genes in immunoprecipitated fractions. Table of differentially expressed protein-coding genes between HET IP and MUT IP samples. DeSeq2 was used to perform differential gene expression analysis between IP samples from these two genotypes and calculate average normalized read counts, log2 fold-change, and *p*-values.

References

Adler, A., Zhao, R., Shin, M. E., Yasuda, R., & Gan, W.-B. (2019). Somatostatin-Expressing Interneurons Enable and Maintain Learning-Dependent Sequential Activation of Pyramidal Neurons. *Neuron*, *102*(1), 202-216.e7. https://doi.org/10.1016/j.neuron.2019.01.036

Alessi, D. R., Saito, Y., Campbell, D. G., Cohen, P., Sithanandam, G., Rapp, U., Ashworth, A., Marshall, C. J., & Cowley, S. (1994). Identification of the sites in MAP kinase kinase-1 phosphorylated by p74raf-1. *The EMBO Journal*, *13*(7), 1610–1619.

Anders, S., Reyes, A., & Huber, W. (2012). Detecting differential usage of exons from RNA-seq data. *Genome Research*, *22*(10), 2008–2017. https://doi.org/10.1101/gr.133744.111

Anderson, T. R., Huguenard, J. R., & Prince, D. A. (2010). Differential effects of Na+-K+ ATPase blockade on cortical layer V neurons. *The Journal of Physiology*, *588*(Pt 22), 4401–4414. https://doi.org/10.1113/jphysiol.2010.191858

Angara, K., Pai, E. L.-L., Bilinovich, S. M., Stafford, A. M., Nguyen, J. T., Li, K. X., Paul, A., Rubenstein, J. L., & Vogt, D. (2020). Nf1 deletion results in depletion of the Lhx6 transcription factor and a specific loss of parvalbumin+ cortical interneurons. *Proceedings of the National Academy of Sciences*, *117*(11), 6189–6195. https://doi.org/10.1073/pnas.1915458117

Assimacopoulos, S., Grove, E. A., & Ragsdale, C. W. (2003). Identification of a *Pax6* -Dependent Epidermal Growth Factor Family Signaling Source at the Lateral Edge of the Embryonic Cerebral Cortex. *The Journal of Neuroscience*, *23*(16), 6399–6403. https://doi.org/10.1523/JNEUROSCI.23-16-06399.2003

Banks, W. A., Schally, A. V., Barrera, C. M., Fasold, M. B., Durham, D. A., Csernus, V. J., Groot, K., & Kastin, A. J. (1990). Permeability of the murine blood-brain barrier to some octapeptide analogs of somatostatin. *Proceedings of the National Academy of Sciences*, *87*(17), 6762–6766. https://doi.org/10.1073/pnas.87.17.6762

Baraban, S. C., & Tallent, M. K. (2004). Interneuron Diversity series: Interneuronal neuropeptides – endogenous regulators of neuronal excitability. *Trends in Neurosciences*, *27*(3), 135–142. https://doi.org/10.1016/j.tins.2004.01.008

Batista-Brito, R., Machold, R., Klein, C., & Fishell, G. (2008). Gene Expression in Cortical Interneuron Precursors is Prescient of their Mature Function. *Cerebral Cortex*, *18*(10), 2306–2317. https://doi.org/10.1093/cercor/bhm258

Ben-Ari, Y., Gaiarsa, J.-L., Tyzio, R., & Khazipov, R. (2007). GABA: A Pioneer Transmitter That Excites Immature Neurons and Generates Primitive Oscillations. *Physiological Reviews*, *87*(4), 1215–1284. https://doi.org/10.1152/physrev.00017.2006

Ben-Shachar, S., Ou, Z., Shaw, C. A., Belmont, J. W., Patel, M. S., Hummel, M., Amato, S., Tartaglia, N., Berg, J., Sutton, V. R., Lalani, S. R., Chinault, A. C., Cheung, S. W., Lupski, J. R., & Patel, A. (2008). 22q11.2 Distal Deletion: A Recurrent Genomic Disorder Distinct from DiGeorge Syndrome and Velocardiofacial Syndrome. *The American Journal of Human Genetics*, *82*(1), 214–221. https://doi.org/10.1016/j.ajhg.2007.09.014

Bitzenhofer, S. H., Pöpplau, J. A., Chini, M., Marquardt, A., & Hanganu-Opatz, I. L. (2021). A transient developmental increase in prefrontal activity alters network maturation and causes cognitive dysfunction in adult mice. *Neuron*, *109*(8), 1350-1364.e6. https://doi.org/10.1016/j.neuron.2021.02.011

Blizinsky, K. D., Diaz-Castro, B., Forrest, M. P., Schürmann, B., Bach, A. P., Martin-de-Saavedra, M. D., Wang, L., Csernansky, J. G., Duan, J., & Penzes, P. (2016). Reversal of dendritic phenotypes in 16p11.2 microduplication mouse model neurons by pharmacological targeting of a network hub. *Proceedings of the National Academy of Sciences*, *113*(30), 8520–8525. https://doi.org/10.1073/pnas.1607014113

Bomkamp, C., Tripathy, S. J., Bengtsson Gonzales, C., Hjerling-Leffler, J., Craig, A. M., & Pavlidis, P. (2019). Transcriptomic correlates of electrophysiological and morphological diversity within and

across excitatory and inhibitory neuron classes. *PLOS Computational Biology*, *15*(6), e1007113. https://doi.org/10.1371/journal.pcbi.1007113

Breunig, J. J., Levy, R., Antonuk, C. D., Molina, J., Dutra-Clarke, M., Park, H., Akhtar, A. A., Kim, G. B., Town, T., Hu, X., Bannykh, S. I., Verhaak, R. G. W., & Danielpour, M. (2015). Ets Factors Regulate Neural Stem Cell Depletion and Gliogenesis in Ras Pathway Glioma. *Cell Reports*, *12*(2), 258–271. https://doi.org/10.1016/j.celrep.2015.06.012

Bueno, O. F. (2000). The MEK1-ERK1/2 signaling pathway promotes compensated cardiac hypertrophy in transgenic mice. *The EMBO Journal*, *19*(23), 6341–6350. https://doi.org/10.1093/emboj/19.23.6341

Cancedda, L., Fiumelli, H., Chen, K., & Poo, M. -m. (2007). Excitatory GABA Action Is Essential for Morphological Maturation of Cortical Neurons In Vivo. *Journal of Neuroscience*, *27*(19), 5224–5235. https://doi.org/10.1523/JNEUROSCI.5169-06.2007

Chen, K., Yang, G., So, K.-F., & Zhang, L. (2019). Activation of Cortical Somatostatin Interneurons Rescues Synapse Loss and Motor Deficits after Acute MPTP Infusion. *IScience*, *17*, 230–241. https://doi.org/10.1016/j.isci.2019.06.040

Choveau, F. S., Abderemane-Ali, F., Coyan, F. C., Es-Salah-Lamoureux, Z., Baró, I., & Loussouarn, G. (2012). Opposite Effects of the S4–S5 Linker and PIP2 on Voltage-Gated Channel Function: KCNQ1/KCNE1 and Other Channels. *Frontiers in Pharmacology*, *3*. https://doi.org/10.3389/fphar.2012.00125

Close, J., Xu, H., De Marco Garcia, N., Batista-Brito, R., Rossignol, E., Rudy, B., & Fishell, G. (2012). Satb1 Is an Activity-Modulated Transcription Factor Required for the Terminal Differentiation and Connectivity of Medial Ganglionic Eminence-Derived Cortical Interneurons. *Journal of Neuroscience*, *32*(49), 17690–17705. https://doi.org/10.1523/JNEUROSCI.3583-12.2012

Cohen, S. M., Ma, H., Kuchibhotla, K. V., Watson, B. O., Buzsáki, G., Froemke, R. C., & Tsien, R. W. (2016). Excitation-Transcription Coupling in Parvalbumin-Positive Interneurons Employs a

Novel CaM Kinase-Dependent Pathway Distinct from Excitatory Neurons. *Neuron*, *90*(2), 292–307. https://doi.org/10.1016/j.neuron.2016.03.001

Courchesne, E., Gazestani, V. H., & Lewis, N. E. (2020). Prenatal Origins of ASD: The When, What, and How of ASD Development. *Trends in Neurosciences*, *43*(5), 326–342. https://doi.org/10.1016/j.tins.2020.03.005

Cowley, S. (1994). Activation of MAP kinase kinase is necessary and sufficient for PC12 differentiation and for transformation of NIH 3T3 cells. *Cell*, *77*(6), 841–852. https://doi.org/10.1016/0092-8674(94)90133-3

Cristo, G. D., Berardi, N., Cancedda, L., Pizzorusso, T., Putignano, E., Ratto, G. M., & Maffei, L. (2001). Requirement of ERK Activation for Visual Cortical Plasticity. *Science*, *292*(5525), 2337–2340. https://doi.org/10.1126/science.1059075

Cummings, K. A., & Clem, R. L. (2020). Prefrontal somatostatin interneurons encode fear memory. *Nature Neuroscience*, *23*(1), 61–74. https://doi.org/10.1038/s41593-019-0552-7

Davies, P., Katzman, R., & Terry, R. D. (1980). Reduced somatostatin-like immunoreactivity in cerebral cortex from cases of Alzheimer disease and Alzheimer senile dementa. *Nature*, *288*(5788), 279–280. https://doi.org/10.1038/288279a0

De Marco García, N. V., Karayannis, T., & Fishell, G. (2011). Neuronal activity is required for the development of specific cortical interneuron subtypes. *Nature*, *472*(7343), 351–355. https://doi.org/10.1038/nature09865

DeFelipe, J., López-Cruz, P. L., Benavides-Piccione, R., Bielza, C., Larrañaga, P., Anderson, S., Burkhalter, A., Cauli, B., Fairén, A., Feldmeyer, D., Fishell, G., Fitzpatrick, D., Freund, T. F., González-Burgos, G., Hestrin, S., Hill, S., Hof, P. R., Huang, J., Jones, E. G., … Ascoli, G. A. (2013). New insights into the classification and nomenclature of cortical GABAergic interneurons. *Nature Reviews Neuroscience*, *14*(3), 202–216. https://doi.org/10.1038/nrn3444

Dehorter, N., Ciceri, G., Bartolini, G., Lim, L., del Pino, I., & Marín, O. (2015). Tuning of fast-spiking interneuron properties by an activity-dependent transcriptional switch. *Science*, *349*(6253), 1216–1220. https://doi.org/10.1126/science.aab3415

del Rio, J., de Lecea, L., Ferrer, I., & Soriano, E. (1994). The development of parvalbumin-immunoreactivity in the neocortex of the mouse. *Developmental Brain Research*, *81*(2), 247–259. https://doi.org/10.1016/0165-3806(94)90311-5

Denaxa, M., Kalaitzidou, M., Garefalaki, A., Achimastou, A., Lasrado, R., Maes, T., & Pachnis, V. (2012). Maturation-Promoting Activity of SATB1 in MGE-Derived Cortical Interneurons. *Cell Reports*, *2*(5), 1351–1362. https://doi.org/10.1016/j.celrep.2012.10.003

Denaxa, M., Neves, G., Rabinowitz, A., Kemlo, S., Liodis, P., Burrone, J., & Pachnis, V. (2018). Modulation of Apoptosis Controls Inhibitory Interneuron Number in the Cortex. *Cell Reports*, *22*(7), 1710–1721. https://doi.org/10.1016/j.celrep.2018.01.064

Dinh Duong, T. A., Hoshiba, Y., Saito, K., Kawasaki, K., Ichikawa, Y., Matsumoto, N., Shinmyo, Y., & Kawasaki, H. (2019). FGF Signaling Directs the Cell Fate Switch from Neurons to Astrocytes in the Developing Mouse Cerebral Cortex. *The Journal of Neuroscience*, *39*(31), 6081–6094. https://doi.org/10.1523/JNEUROSCI.2195-18.2019

Dobin, A., Davis, C. A., Schlesinger, F., Drenkow, J., Zaleski, C., Jha, S., Batut, P., Chaisson, M., & Gingeras, T. R. (2013). STAR: Ultrafast universal RNA-seq aligner. *Bioinformatics (Oxford, England)*, *29*(1), 15–21. https://doi.org/10.1093/bioinformatics/bts635

Edgar, R., Domrachev, M., & Lash, A. E. (2002). Gene Expression Omnibus: NCBI gene expression and hybridization array data repository. *Nucleic Acids Research*, *30*(1), 207–210. https://doi.org/10.1093/nar/30.1.207

Engin, E., & Treit, D. (2009). Anxiolytic and antidepressant actions of somatostatin: The role of sst2 and sst3 receptors. *Psychopharmacology*, *206*(2), 281–289. https://doi.org/10.1007/s00213-009-1605-5

Exposito-Alonso, D., Osório, C., Bernard, C., Pascual-García, S., del Pino, I., Marín, O., & Rico, B. (2020). Subcellular sorting of neuregulins controls the assembly of excitatory-inhibitory cortical circuits. *ELife*, *9*, e57000. https://doi.org/10.7554/eLife.57000

Faedo, A., Borello, U., & Rubenstein, J. L. R. (2010). Repression of Fgf Signaling by Sprouty1-2 Regulates Cortical Patterning in Two Distinct Regions and Times. *Journal of Neuroscience*, *30*(11), 4015–4023. https://doi.org/10.1523/JNEUROSCI.0307-10.2010

Fazzari, P., Paternain, A. V., Valiente, M., Pla, R., Luján, R., Lloyd, K., Lerma, J., Marín, O., & Rico, B. (2010). Control of cortical GABA circuitry development by Nrg1 and ErbB4 signalling. *Nature*, *464*(7293), 1376–1380. https://doi.org/10.1038/nature08928

Fee, C., Banasr, M., & Sibille, E. (2017). Somatostatin-Positive Gamma-Aminobutyric Acid Interneuron Deficits in Depression: Cortical Microcircuit and Therapeutic Perspectives. *Biological Psychiatry*, *82*(8), 549–559. https://doi.org/10.1016/j.biopsych.2017.05.024

Fernandez, B. A., Roberts, W., Chung, B., Weksberg, R., Meyn, S., Szatmari, P., Joseph-George, A. M., MacKay, S., Whitten, K., Noble, B., Vardy, C., Crosbie, V., Luscombe, S., Tucker, E., Turner, L., Marshall, C. R., & Scherer, S. W. (2010). Phenotypic spectrum associated with de novo and inherited deletions and duplications at 16p11.2 in individuals ascertained for diagnosis of autism spectrum disorder. *Journal of Medical Genetics*, *47*(3), 195–203. https://doi.org/10.1136/jmg.2009.069369

Filges, I., Sparagana, S., Sargent, M., Selby, K., Schlade-Bartusiak, K., Lueder, G. T., Robichaux-Viehoever, A., Schlaggar, B. L., Shimony, J. S., & Shinawi, M. (2014). Brain MRI abnormalities and spectrum of neurological and clinical findings in three patients with proximal 16p11.2 microduplication. *American Journal of Medical Genetics. Part A*, *164A*(8), 2003–2012. https://doi.org/10.1002/ajmg.a.36605

Forloni, G., Hohmann, C., & Coyle, J. T. (1990). Developmental expression of somatostatin in mouse brain. I. Immunocytochemical studies. *Developmental Brain Research*, *53*(1), 6–25. https://doi.org/10.1016/0165-3806(90)90120-N

Fu, Y., Tucciarone, J. M., Espinosa, J. S., Sheng, N., Darcy, D. P., Nicoll, R. A., Huang, Z. J., & Stryker, M. P. (2014). A cortical circuit for gain control by behavioral state. *Cell*, *156*(6), 1139–1152. https://doi.org/10.1016/j.cell.2014.01.050

Fyffe-Maricich, S. L., Karlo, J. C., Landreth, G. E., & Miller, R. H. (2011). The ERK2 Mitogen-Activated Protein Kinase Regulates the Timing of Oligodendrocyte Differentiation. *Journal of Neuroscience*, *31*(3), 843–850. https://doi.org/10.1523/JNEUROSCI.3239-10.2011

Glorioso, C., Sabatini, M., Unger, T., Hashimoto, T., Monteggia, L. M., Lewis, D. A., & Mirnics, K. (2006). Specificity and timing of neocortical transcriptome changes in response to BDNF gene ablation during embryogenesis or adulthood. *Molecular Psychiatry*, *11*(7), 633–648. https://doi.org/10.1038/sj.mp.4001835

Goddeyne, C., Nichols, J., Wu, C., & Anderson, T. (2015). Repetitive mild traumatic brain injury induces ventriculomegaly and cortical thinning in juvenile rats. *Journal of Neurophysiology*, *113*(9), 3268–3280. https://doi.org/10.1152/jn.00970.2014

Gour, A., Boergens, K. M., Heike, N., Hua, Y., Laserstein, P., Song, K., & Helmstaedter, M. (2021). Postnatal connectomic development of inhibition in mouse barrel cortex. *Science*, *371*(6528), eabb4534. https://doi.org/10.1126/science.abb4534

Grilli, M., Raiteri, L., & Pittaluga, A. (2004). Somatostatin inhibits glutamate release from mouse cerebrocortical nerve endings through presynaptic sst2 receptors linked to the adenylyl cyclase–protein kinase A pathway. *Neuropharmacology*, *46*(3), 388–396. https://doi.org/10.1016/j.neuropharm.2003.09.012

Guenthner, C. J., Miyamichi, K., Yang, H. H., Heller, H. C., & Luo, L. (2013). Permanent Genetic Access to Transiently Active Neurons via TRAP: Targeted Recombination in Active Populations. *Neuron*, *78*(5), 773–784. https://doi.org/10.1016/j.neuron.2013.03.025

Gutmann, D. H., Wu, Y. L., Hedrick, N. M., Zhu, Y., Guha, A., & Parada, L. F. (2001). Heterozygosity for the neurofibromatosis 1 (NF1) tumor suppressor results in abnormalities in cell attachment,

spreading and motility in astrocytes. *Human Molecular Genetics*, *10*(26), 3009–3016. https://doi.org/10.1093/hmg/10.26.3009

Hanson, E., Armbruster, M., Lau, L. A., Sommer, M. E., Klaft, Z.-J., Swanger, S. A., Traynelis, S. F., Moss, S. J., Noubary, F., Chadchankar, J., & Dulla, C. G. (2019). Tonic Activation of GluN2C/GluN2D-Containing NMDA Receptors by Ambient Glutamate Facilitates Cortical Interneuron Maturation. *The Journal of Neuroscience: The Official Journal of the Society for Neuroscience*, *39*(19), 3611–3626. https://doi.org/10.1523/JNEUROSCI.1392-18.2019

Heavner, W. E., & Smith, S. E. P. (2020). Resolving the Synaptic versus Developmental Dichotomy of Autism Risk Genes. *Trends in Neurosciences*, *43*(4), 227–241. https://doi.org/10.1016/j.tins.2020.01.009

Holter, M. C., Hewitt, L. T., Nishimura, K. J., Knowles, S. J., Bjorklund, G. R., Shah, S., Fry, N. R., Rees, K. P., Gupta, T. A., Daniels, C. W., Li, G., Marsh, S., Treiman, D. M., Olive, M. F., Anderson, T. R., Sanabria, F., Snider, W. D., & Newbern, J. M. (2021). Hyperactive MEK1 Signaling in Cortical GABAergic Neurons Promotes Embryonic Parvalbumin Neuron Loss and Defects in Behavioral Inhibition. *Cerebral Cortex*, bhaa413. https://doi.org/10.1093/cercor/bhaa413

Holter, M. C., Hewitt, Lauren. T., Koebele, S. V., Judd, J. M., Xing, L., Bimonte-Nelson, H. A., Conrad, C. D., Araki, T., Neel, B. G., Snider, W. D., & Newbern, J. M. (2019). The Noonan Syndrome-linked Raf1L613V mutation drives increased glial number in the mouse cortex and enhanced learning. *PLOS Genetics*, *15*(4), e1008108. https://doi.org/10.1371/journal.pgen.1008108

Hong, E. J., McCord, A. E., & Greenberg, M. E. (2008). A Biological Function for the Neuronal Activity-Dependent Component of Bdnf Transcription in the Development of Cortical Inhibition. *Neuron*, *60*(4), 610–624. https://doi.org/10.1016/j.neuron.2008.09.024

Hrvatin, S., Hochbaum, D. R., Nagy, M. A., Cicconet, M., Robertson, K., Cheadle, L., Zilionis, R., Ratner, A., Borges-Monroy, R., Klein, A. M., Sabatini, B. L., & Greenberg, M. E. (2018). Single-

cell analysis of experience-dependent transcriptomic states in the mouse visual cortex. *Nature Neuroscience*, *21*(1), 120–129. https://doi.org/10.1038/s41593-017-0029-5

Hu, J. S., Vogt, D., Sandberg, M., & Rubenstein, J. L. (2017). Cortical interneuron development: A tale of time and space. *Development*, *144*(21), 3867–3878. https://doi.org/10.1242/dev.132852

Huang, Z. J., Kirkwood, A., Pizzorusso, T., Porciatti, V., Morales, B., Bear, M. F., Maffei, L., & Tonegawa, S. (1999). BDNF Regulates the Maturation of Inhibition and the Critical Period of Plasticity in Mouse Visual Cortex. *Cell*, *98*(6), 739–755. https://doi.org/10.1016/S0092-8674(00)81509-3

Hutton, S. R., Otis, J. M., Kim, E. M., Lamsal, Y., Stuber, G. D., & Snider, W. D. (2017). ERK/MAPK Signaling Is Required for Pathway-Specific Striatal Motor Functions. *The Journal of Neuroscience: The Official Journal of the Society for Neuroscience*, *37*(34), 8102–8115. https://doi.org/10.1523/JNEUROSCI.0473-17.2017

Itami, C., Kimura, F., & Nakamura, S. (2007). Brain-Derived Neurotrophic Factor Regulates the Maturation of Layer 4 Fast-Spiking Cells after the Second Postnatal Week in the Developing Barrel Cortex. *Journal of Neuroscience*, *27*(9), 2241–2252. https://doi.org/10.1523/JNEUROSCI.3345-06.2007

Jendryka, M., Palchaudhuri, M., Ursu, D., van der Veen, B., Liss, B., Kätzel, D., Nissen, W., & Pekcec, A. (2019). Pharmacokinetic and pharmacodynamic actions of clozapine-N-oxide, clozapine, and compound 21 in DREADD-based chemogenetics in mice. *Scientific Reports*, *9*(1), 4522. https://doi.org/10.1038/s41598-019-41088-2

Kaneko, K., Currin, C. B., Goff, K. M., Wengert, E. R., Somarowthu, A., Vogels, T. P., & Goldberg, E. M. (2022). Developmentally regulated impairment of parvalbumin interneuron synaptic transmission in an experimental model of Dravet syndrome. *Cell Reports*, *38*(13), 110580. https://doi.org/10.1016/j.celrep.2022.110580

Kawaguchi, Y. (1997). GABAergic cell subtypes and their synaptic connections in rat frontal cortex. *Cerebral Cortex*, *7*(6), 476–486. https://doi.org/10.1093/cercor/7.6.476

Kessaris, N., Fogarty, M., Iannarelli, P., Grist, M., Wegner, M., & Richardson, W. D. (2006). Competing waves of oligodendrocytes in the forebrain and postnatal elimination of an embryonic lineage. *Nature Neuroscience*, *9*(2), 173–179. https://doi.org/10.1038/nn1620

Kiviniemi, A., Gardberg, M., Frantzén, J., Pesola, M., Vuorinen, V., Parkkola, R., Tolvanen, T., Suilamo, S., Johansson, J., Luoto, P., Kemppainen, J., Roivainen, A., & Minn, H. (2015). Somatostatin receptor subtype 2 in high-grade gliomas: PET/CT with 68Ga-DOTA-peptides, correlation to prognostic markers, and implications for targeted radiotherapy. *EJNMMI Research*, *5*(1), 25. https://doi.org/10.1186/s13550-015-0106-2

Klesse, L. J., Meyers, K. A., Marshall, C. J., & Parada, L. F. (1999). Nerve growth factor induces survival and differentiation through two distinct signaling cascades in PC12 cells. *Oncogene*, *18*(12), 2055–2068. https://doi.org/10.1038/sj.onc.1202524

Kluge, C., Stoppel, C., Szinyei, C., Stork, O., & Pape, H.-C. (2008). Role of the somatostatin system in contextual fear memory and hippocampal synaptic plasticity. *Learning & Memory*, *15*(4), 252–260. https://doi.org/10.1101/lm.793008

Krencik, R., Hokanson, K. C., Narayan, A. R., Dvornik, J., Rooney, G. E., Rauen, K. A., Weiss, L. A., Rowitch, D. H., & Ullian, E. M. (2015). Dysregulation of astrocyte extracellular signaling in Costello syndrome. *Science Translational Medicine*, *7*(286), 286ra66. https://doi.org/10.1126/scitranslmed.aaa5645

Krenz, M., Gulick, J., Osinska, H. E., Colbert, M. C., Molkentin, J. D., & Robbins, J. (2008). Role of ERK1/2 signaling in congenital valve malformations in Noonan syndrome. *Proceedings of the National Academy of Sciences*, *105*(48), 18930–18935. https://doi.org/10.1073/pnas.0806556105

Lajiness, J. D., Snider, P., Wang, J., Feng, G.-S., Krenz, M., & Conway, S. J. (2014). SHP-2 deletion in postmigratory neural crest cells results in impaired cardiac sympathetic innervation. *Proceedings of the National Academy of Sciences*, *111*(14), E1374–E1382. https://doi.org/10.1073/pnas.1319208111

Lavoie, H., Gagnon, J., & Therrien, M. (2020). ERK signalling: A master regulator of cell behaviour, life and fate. *Nature Reviews Molecular Cell Biology*, *21*(10), 607–632. https://doi.org/10.1038/s41580-020-0255-7

Lee, C., Harkin, E. F., Yin, X., Naud, R., & Chen, S. (2022). Cell-type-specific responses to associative learning in the primary motor cortex. *ELife*, *11*, e72549. https://doi.org/10.7554/eLife.72549

Lee, D. R., Rhodes, C., Mitra, A., Zhang, Y., Maric, D., Dale, R. K., & Petros, T. J. (2022). Transcriptional heterogeneity of ventricular zone cells in the ganglionic eminences of the mouse forebrain. *ELife*, *11*, e71864. https://doi.org/10.7554/eLife.71864

Li, S., Mattar, P., Dixit, R., Lawn, S. O., Wilkinson, G., Kinch, C., Eisenstat, D., Kurrasch, D. M., Chan, J. A., & Schuurmans, C. (2014). RAS/ERK Signaling Controls Proneural Genetic Programs in Cortical Development and Gliomagenesis. *Journal of Neuroscience*, *34*(6), 2169–2190. https://doi.org/10.1523/JNEUROSCI.4077-13.2014

Li, X., Newbern, J. M., Wu, Y., Morgan-Smith, M., Zhong, J., Charron, J., & Snider, W. D. (2012). MEK Is a Key Regulator of Gliogenesis in the Developing Brain. *Neuron*, *75*(6), 1035–1050. https://doi.org/10.1016/j.neuron.2012.08.031

Liguz-Lecznar, M., Urban-Ciecko, J., & Kossut, M. (2016). Somatostatin and Somatostatin-Containing Neurons in Shaping Neuronal Activity and Plasticity. *Frontiers in Neural Circuits*, *10*. https://doi.org/10.3389/fncir.2016.00048

Lim, L., Mi, D., Llorca, A., & Marín, O. (2018). Development and Functional Diversification of Cortical Interneurons. *Neuron*, *100*(2), 294–313. https://doi.org/10.1016/j.neuron.2018.10.009

Linhares, N. D., Freire, M. C. M., Cardenas, R. G. C. do C. L., Pena, H. B., Lachlan, K., Dallapiccola, B., Bacino, C., Delobel, B., James, P., Thuresson, A.-C., Annerén, G., & Pena, S. D. J. (2016). 1p13.2 deletion displays clinical features overlapping Noonan syndrome, likely related to NRAS gene haploinsufficiency. *Genetics and Molecular Biology*, *39*(3), 349–357. https://doi.org/10.1590/1678-4685-GMB-2016-0049

Lodato, S., Rouaux, C., Quast, K. B., Jantrachotechatchawan, C., Studer, M., Hensch, T. K., & Arlotta, P. (2011). Excitatory Projection Neuron Subtypes Control the Distribution of Local Inhibitory Interneurons in the Cerebral Cortex. *Neuron*, *69*(4), 763–779. https://doi.org/10.1016/j.neuron.2011.01.015

Lord, C., Brugha, T. S., Charman, T., Cusack, J., Dumas, G., Frazier, T., Jones, E. J. H., Jones, R. M., Pickles, A., State, M. W., Taylor, J. L., & Veenstra-VanderWeele, J. (2020). Autism spectrum disorder. *Nature Reviews Disease Primers*, *6*(1), 5. https://doi.org/10.1038/s41572-019-0138-4

Love, M. I., Huber, W., & Anders, S. (2014). Moderated estimation of fold change and dispersion for RNA-seq data with DESeq2. *Genome Biology*, *15*(12), 550. https://doi.org/10.1186/s13059-014-0550-8

Madisen, L., Zwingman, T. A., Sunkin, S. M., Oh, S. W., Zariwala, H. A., Gu, H., Ng, L. L., Palmiter, R. D., Hawrylycz, M. J., Jones, A. R., Lein, E. S., & Zeng, H. (2010). A robust and high-throughput Cre reporting and characterization system for the whole mouse brain. *Nature Neuroscience*, *13*(1), 133–140. https://doi.org/10.1038/nn.2467

Magno, L., Asgarian, Z., Pendolino, V., Velona, T., Mackintosh, A., Lee, F., Stryjewska, A., Zimmer, C., Guillemot, F., Farrant, M., Clark, B., & Kessaris, N. (2021). Transient developmental imbalance of cortical interneuron subtypes presages long-term changes in behavior. *Cell Reports*, *35*(11), 109249. https://doi.org/10.1016/j.celrep.2021.109249

Maisonpierre, P. C., Belluscio, L., Friedman, B., Alderson, R. F., Wiegand, S. J., Furth, M. E., Lindsay, R. M., & Yancopoulos, G. D. (1990). NT-3, BDNF, and NGF in the developing rat nervous system: Parallel as well as reciprocal patterns of expression. *Neuron*, *5*(4), 501–509. https://doi.org/10.1016/0896-6273(90)90089-X

Malik, R., Pai, E. L.-L., Rubin, A. N., Stafford, A. M., Angara, K., Minasi, P., Rubenstein, J. L., Sohal, V. S., & Vogt, D. (2019). Tsc1 represses parvalbumin expression and fast-spiking properties in somatostatin lineage cortical interneurons. *Nature Communications*, *10*(1), 4994. https://doi.org/10.1038/s41467-019-12962-4

Mardinly, A. R., Spiegel, I., Patrizi, A., Centofante, E., Bazinet, J. E., Tzeng, C. P., Mandel-Brehm, C., Harmin, D. A., Adesnik, H., Fagiolini, M., & Greenberg, M. E. (2016). Sensory experience regulates cortical inhibition by inducing IGF1 in VIP neurons. *Nature*, *531*(7594), 371–375. https://doi.org/10.1038/nature17187

Marsh, E. D., Nasrallah, M. P., Walsh, C., Murray, K. A., Nicole Sunnen, C., McCoy, A., & Golden, J. A. (2016). Developmental interneuron subtype deficits after targeted loss of Arx. *BMC Neuroscience*, *17*(1), 35. https://doi.org/10.1186/s12868-016-0265-8

Martin, D., Xu, J., Porretta, C., & Nichols, C. D. (2017). Neurocytometry: Flow Cytometric Sorting of Specific Neuronal Populations from Human and Rodent Brain. *ACS Chemical Neuroscience*, *8*(2), 356–367. https://doi.org/10.1021/acschemneuro.6b00374

Matthews, R. P., Guthrie, C. R., Wailes, L. M., Zhao, X., Means, A. R., & McKnight, G. S. (1994). Calcium/calmodulin-dependent protein kinase types II and IV differentially regulate CREB-dependent gene expression. *Molecular and Cellular Biology*, *14*(9), 6107–6116. https://doi.org/10.1128/MCB.14.9.6107

Mayer, C., Hafemeister, C., Bandler, R. C., Machold, R., Batista Brito, R., Jaglin, X., Allaway, K., Butler, A., Fishell, G., & Satija, R. (2018). Developmental diversification of cortical inhibitory interneurons. *Nature*, *555*(7697), 457–462. https://doi.org/10.1038/nature25999

McCormick, D. A., Connors, B. W., Lighthall, J. W., & Prince, D. A. (1985). Comparative electrophysiology of pyramidal and sparsely spiny stellate neurons of the neocortex. *Journal of Neurophysiology*, *54*(4), 782–806. https://doi.org/10.1152/jn.1985.54.4.782

McKeage, K. (2015). Pasireotide in Acromegaly: A Review. *Drugs*, *75*(9), 1039–1048. https://doi.org/10.1007/s40265-015-0413-y

McKenzie, M. G., Cobbs, L. V., Dummer, P. D., Petros, T. J., Halford, M. M., Stacker, S. A., Zou, Y., Fishell, G. J., & Au, E. (2019). Non-canonical Wnt Signaling through Ryk Regulates the Generation of Somatostatin- and Parvalbumin-Expressing Cortical Interneurons. *Neuron*, *103*(5), 853-864.e4. https://doi.org/10.1016/j.neuron.2019.06.003

Mi, D., Li, Z., Lim, L., Li, M., Moissidis, M., Yang, Y., Gao, T., Hu, T. X., Pratt, T., Price, D. J., Sestan, N., & Marín, O. (2018). Early emergence of cortical interneuron diversity in the mouse embryo. *Science*, *360*(6384), 81–85. https://doi.org/10.1126/science.aar6821

Miller, M. N., Okaty, B. W., Kato, S., & Nelson, S. B. (2011). Activity-dependent changes in the firing properties of neocortical fast-spiking interneurons in the absence of large changes in gene expression. *Developmental Neurobiology*, *71*(1), 62–70. https://doi.org/10.1002/dneu.20811

Minocha, S., Valloton, D., Ypsilanti, A. R., Fiumelli, H., Allen, E. A., Yanagawa, Y., Marin, O., Chédotal, A., Hornung, J.-P., & Lebrand, C. (2015). Nkx2.1-derived astrocytes and neurons together with Slit2 are indispensable for anterior commissure formation. *Nature Communications*, *6*, 6887. https://doi.org/10.1038/ncomms7887

Miyoshi, G., Butt, S. J. B., Takebayashi, H., & Fishell, G. (2007). Physiologically Distinct Temporal Cohorts of Cortical Interneurons Arise from Telencephalic Olig2-Expressing Precursors. *Journal of Neuroscience*, *27*(29), 7786–7798. https://doi.org/10.1523/JNEUROSCI.1807-07.2007

Monory, K., Massa, F., Egertová, M., Eder, M., Blaudzun, H., Westenbroek, R., Kelsch, W., Jacob, W., Marsch, R., Ekker, M., Long, J., Rubenstein, J. L., Goebbels, S., Nave, K.-A., During, M., Klugmann, M., Wölfel, B., Dodt, H.-U., Zieglgänsberger, W., … Lutz, B. (2006). The Endocannabinoid System Controls Key Epileptogenic Circuits in the Hippocampus. *Neuron*, *51*(4), 455–466. https://doi.org/10.1016/j.neuron.2006.07.006

Montminy, M. R., & Bilezikjian, L. M. (1987). Binding of a nuclear protein to the cyclic-AMP response element of the somatostatin gene. *Nature*, *328*(6126), 175–178. https://doi.org/10.1038/328175a0

Mori, M. X., Itsuki, K., Hase, H., Sawamura, S., Kurokawa, T., Mori, Y., & Inoue, R. (2015). Dynamics of receptor-operated Ca2+ currents through TRPC channels controlled via the PI(4,5)P2-PLC signaling pathway. *Frontiers in Pharmacology*, *6*. https://doi.org/10.3389/fphar.2015.00022

Moyses-Oliveira, M., Yadav, R., Erdin, S., & Talkowski, M. E. (2020). New gene discoveries highlight functional convergence in autism and related neurodevelopmental disorders. *Current Opinion in Genetics & Development*, *65*, 195–206. https://doi.org/10.1016/j.gde.2020.07.001

Munguba, H., Nikouei, K., Hochgerner, H., Oberst, P., Kouznetsova, A., Ryge, J., Batista-Brito, R., Munoz-Manchado, A. B., Close, J., Linnarsson, S., & Hjerling-Leffler, J. (2019). *Transcriptional maintenance of cortical somatostatin interneuron subtype identity during migration* [Preprint]. Neuroscience. https://doi.org/10.1101/593285

Nawaratne, V., Leach, K., Suratman, N., Loiacono, R. E., Felder, C. C., Armbruster, B. N., Roth, B. L., Sexton, P. M., & Christopoulos, A. (2008). New Insights into the Function of M_4 Muscarinic Acetylcholine Receptors Gained Using a Novel Allosteric Modulator and a DREADD (Designer Receptor Exclusively Activated by a Designer Drug). *Molecular Pharmacology*, *74*(4), 1119–1131. https://doi.org/10.1124/mol.108.049353

Neves, G., Shah, M. M., Liodis, P., Achimastou, A., Denaxa, M., Roalfe, G., Sesay, A., Walker, M. C., & Pachnis, V. (2013). The LIM Homeodomain Protein Lhx6 Regulates Maturation of Interneurons and Network Excitability in the Mammalian Cortex. *Cerebral Cortex*, *23*(8), 1811–1823. https://doi.org/10.1093/cercor/bhs159

Newbern, J., Li, X., Shoemaker, S. E., Zhou, J., Zhong, J., Wu, Y., Bonder, D., Hollenback, S., Coppola, G., Geschwind, D. H., Landreth, G. E., & Snider, W. D. (2011). Specific functions for ERK/MAPK signaling during PNS development. *Neuron*, *69*(1), 91–105. https://doi.org/10.1016/j.neuron.2010.12.003

Newbern, J., Zhong, J., Wickramasinghe, R. S., Li, X., Wu, Y., Samuels, I., Cherosky, N., Karlo, J. C., O'Loughlin, B., Wikenheiser, J., Gargesha, M., Doughman, Y. Q., Charron, J., Ginty, D. D., Watanabe, M., Saitta, S. C., Snider, W. D., & Landreth, G. E. (2008). Mouse and human phenotypes indicate a critical conserved role for ERK2 signaling in neural crest development. *Proceedings of the National Academy of Sciences of the United States of America*, *105*(44), 17115–17120. https://doi.org/10.1073/pnas.0805239105

Nichols, J., Bjorklund, G. R., Newbern, J., & Anderson, T. (2018). Parvalbumin fast-spiking interneurons are selectively altered by paediatric traumatic brain injury. *The Journal of Physiology*, *596*(7), 1277–1293. https://doi.org/10.1113/JP275393

Nigro, M. J., Hashikawa-Yamasaki, Y., & Rudy, B. (2018). Diversity and Connectivity of Layer 5 Somatostatin-Expressing Interneurons in the Mouse Barrel Cortex. *The Journal of Neuroscience*, *38*(7), 1622–1633. https://doi.org/10.1523/JNEUROSCI.2415-17.2017

Nowaczyk, M. J. M., Thompson, B. A., Zeesman, S., Moog, U., Sanchez-Lara, P. A., Magoulas, P. L., Falk, R. E., Hoover-Fong, J. E., Batista, D. A. S., Amudhavalli, S. M., White, S. M., Graham, G. E., & Rauen, K. A. (2014). Deletion of MAP2K2/MEK2: A novel mechanism for a RASopathy? *Clinical Genetics*, *85*(2), 138–146. https://doi.org/10.1111/cge.12116

Obrietan, K., Gao, X.-B., & van den Pol, A. N. (2002). Excitatory Actions of GABA Increase BDNF Expression via a MAPK-CREB–Dependent Mechanism—A Positive Feedback Circuit in Developing Neurons. *Journal of Neurophysiology*, *88*(2), 1005–1015. https://doi.org/10.1152/jn.2002.88.2.1005

Oishi, K., Watatani, K., Itoh, Y., Okano, H., Guillemot, F., Nakajima, K., & Gotoh, Y. (2009). Selective induction of neocortical GABAergic neurons by the PDK1-Akt pathway through activation of Mash1. *Proceedings of the National Academy of Sciences*, *106*(31), 13064–13069. https://doi.org/10.1073/pnas.0808400106

Okaty, B. W., Miller, M. N., Sugino, K., Hempel, C. M., & Nelson, S. B. (2009). Transcriptional and Electrophysiological Maturation of Neocortical Fast-Spiking GABAergic Interneurons. *Journal of Neuroscience*, *29*(21), 7040–7052. https://doi.org/10.1523/JNEUROSCI.0105-09.2009

O'Leary, D. D. M., Chou, S.-J., & Sahara, S. (2007). Area Patterning of the Mammalian Cortex. *Neuron*, *56*(2), 252–269. https://doi.org/10.1016/j.neuron.2007.10.010

Ouwenga, R., Lake, A. M., Aryal, S., Lagunas, T., & Dougherty, J. D. (2018). The Differences in Local Translatome across Distinct Neuron Types Is Mediated by Both Baseline Cellular Differences and Post-transcriptional Mechanisms. *Eneuro*, *5*(6), ENEURO.0320-18.2018. https://doi.org/10.1523/ENEURO.0320-18.2018

Owens, D. F., & Kriegstein, A. R. (2002). Is there more to gaba than synaptic inhibition? *Nature Reviews Neuroscience*, *3*(9), 715–727. https://doi.org/10.1038/nrn919

Pan, N. C., Fang, A., Shen, C., Sun, L., Wu, Q., & Wang, X. (2018). Early Excitatory Activity-Dependent Maturation of Somatostatin Interneurons in Cortical Layer 2/3 of Mice. *Cerebral Cortex*. https://doi.org/10.1093/cercor/bhy293

Pantazopoulos, H., Wiseman, J. T., Markota, M., Ehrenfeld, L., & Berretta, S. (2017). Decreased Numbers of Somatostatin-Expressing Neurons in the Amygdala of Subjects With Bipolar Disorder or Schizophrenia: Relationship to Circadian Rhythms. *Biological Psychiatry*, *81*(6), 536–547. https://doi.org/10.1016/j.biopsych.2016.04.006

Paul, A., Crow, M., Raudales, R., He, M., Gillis, J., & Huang, Z. J. (2017). Transcriptional Architecture of Synaptic Communication Delineates GABAergic Neuron Identity. *Cell*, *171*(3), 522-539.e20. https://doi.org/10.1016/j.cell.2017.08.032

Peerboom, C., & Wierenga, C. J. (2021). The postnatal GABA shift: A developmental perspective. *Neuroscience & Biobehavioral Reviews*, *124*, 179–192. https://doi.org/10.1016/j.neubiorev.2021.01.024

Peng, Z., Zhang, N., Wei, W., Huang, C. S., Cetina, Y., Otis, T. S., & Houser, C. R. (2013). A Reorganized GABAergic Circuit in a Model of Epilepsy: Evidence from Optogenetic Labeling and Stimulation of Somatostatin Interneurons. *Journal of Neuroscience*, *33*(36), 14392–14405. https://doi.org/10.1523/JNEUROSCI.2045-13.2013

Petros, T. J., Bultje, R. S., Ross, M. E., Fishell, G., & Anderson, S. A. (2015). Apical versus Basal Neurogenesis Directs Cortical Interneuron Subclass Fate. *Cell Reports*, *13*(6), 1090–1095. https://doi.org/10.1016/j.celrep.2015.09.079

Pietrobono, S., Gagliardi, S., & Stecca, B. (2019). Non-canonical Hedgehog Signaling Pathway in Cancer: Activation of GLI Transcription Factors Beyond Smoothened. *Frontiers in Genetics*, *10*, 556. https://doi.org/10.3389/fgene.2019.00556

Po, A., Silvano, M., Miele, E., Capalbo, C., Eramo, A., Salvati, V., Todaro, M., Besharat, Z. M., Catanzaro, G., Cucchi, D., Coni, S., Di Marcotullio, L., Canettieri, G., Vacca, A., Stassi, G., De Smaele, E., Tartaglia, M., Screpanti, I., De Maria, R., & Ferretti, E. (2017). Noncanonical GLI1

signaling promotes stemness features and in vivo growth in lung adenocarcinoma. *Oncogene*, *36*(32), 4641–4652. https://doi.org/10.1038/onc.2017.91

Polleux, F., Whitford, K. L., Dijkhuizen, P. A., Vitalis, T., & Ghosh, A. (2002). Control of cortical interneuron migration by neurotrophins and PI3-kinase signaling. *Development (Cambridge, England)*, *129*(13), 3147–3160.

Priya, R., Paredes, M. F., Karayannis, T., Yusuf, N., Liu, X., Jaglin, X., Graef, I., Alvarez-Buylla, A., & Fishell, G. (2018). Activity Regulates Cell Death within Cortical Interneurons through a Calcineurin-Dependent Mechanism. *Cell Reports*, *22*(7), 1695–1709. https://doi.org/10.1016/j.celrep.2018.01.007

Pucilowska, J., Puzerey, P. A., Karlo, J. C., Galan, R. F., & Landreth, G. E. (2012). Disrupted ERK Signaling during Cortical Development Leads to Abnormal Progenitor Proliferation, Neuronal and Network Excitability and Behavior, Modeling Human Neuro-Cardio-Facial-Cutaneous and Related Syndromes. *Journal of Neuroscience*, *32*(25), 8663–8677. https://doi.org/10.1523/JNEUROSCI.1107-12.2012

Pucilowska, J., Vithayathil, J., Tavares, E. J., Kelly, C., Karlo, J. C., & Landreth, G. E. (2015). The 16p11.2 Deletion Mouse Model of Autism Exhibits Altered Cortical Progenitor Proliferation and Brain Cytoarchitecture Linked to the ERK MAPK Pathway. *Journal of Neuroscience*, *35*(7), 3190–3200. https://doi.org/10.1523/JNEUROSCI.4864-13.2015

Qureshi, A. Y., Mueller, S., Snyder, A. Z., Mukherjee, P., Berman, J. I., Roberts, T. P. L., Nagarajan, S. S., Spiro, J. E., Chung, W. K., Sherr, E. H., Buckner, R. L., & Simons VIP Consortium. (2014). Opposing brain differences in 16p11.2 deletion and duplication carriers. *The Journal of Neuroscience: The Official Journal of the Society for Neuroscience*, *34*(34), 11199–11211. https://doi.org/10.1523/JNEUROSCI.1366-14.2014

Rauen, K. A. (2013). The RASopathies. *Annual Review of Genomics and Human Genetics*, *14*(1), 355–369. https://doi.org/10.1146/annurev-genom-091212-153523

Reh, R. K., Dias, B. G., Nelson, C. A., Kaufer, D., Werker, J. F., Kolb, B., Levine, J. D., & Hensch, T. K. (2020). Critical period regulation across multiple timescales. *Proceedings of the National Academy of Sciences*, 201820836. https://doi.org/10.1073/pnas.1820836117

Rizvi, T. A., Akunuru, S., de Courten-Myers, G., Switzer, R. C., Nordlund, M. L., & Ratner, N. (1999). Region-specific astrogliosis in brains of mice heterozygous for mutations in the neurofibromatosis type 1 (Nf1) tumor suppressor. *Brain Research*, *816*(1), 111–123. https://doi.org/10.1016/s0006-8993(98)01133-0

Robbins, R. J., Brines, M. L., Kim, J. H., Adrian, T., De Lanerolle, N., Welsh, S., & Spencer, D. D. (1991). A selective loss of somatostatin in the hippocampus of patients with temporal lobe epilepsy. *Annals of Neurology*, *29*(3), 325–332. https://doi.org/10.1002/ana.410290316

Rogan, S. C., & Roth, B. L. (2011). Remote Control of Neuronal Signaling. *Pharmacological Reviews*, *63*(2), 291–315. https://doi.org/10.1124/pr.110.003020

Rogers, S., Rozman, P. A., Valero, M., Doyle, W. K., & Buzsáki, G. (2021). Mechanisms and plasticity of chemogenically induced interneuronal suppression of principal cells. *Proceedings of the National Academy of Sciences*, *118*(2), e2014157118. https://doi.org/10.1073/pnas.2014157118

Rosina, E., Battan, B., Siracusano, M., Di Criscio, L., Hollis, F., Pacini, L., Curatolo, P., & Bagni, C. (2019). Disruption of mTOR and MAPK pathways correlates with severity in idiopathic autism. *Translational Psychiatry*, *9*(1), 50. https://doi.org/10.1038/s41398-018-0335-z

Roth, B. L. (2016). DREADDs for Neuroscientists. *Neuron*, *89*(4), 683–694. https://doi.org/10.1016/j.neuron.2016.01.040

Ryu, H.-H., Kang, M., Park, J., Park, S.-H., & Lee, Y.-S. (2019). Enriched expression of NF1 in inhibitory neurons in both mouse and human brain. *Molecular Brain*, *12*(1), 60. https://doi.org/10.1186/s13041-019-0481-0

Ryu, H.-H., Kim, T., Kim, J.-W., Kang, M., Park, P., Kim, Y. G., Kim, H., Ha, J., Choi, J. E., Lee, J., Lim, C.-S., Kim, C.-H., Kim, S. J., Silva, A. J., Kaang, B.-K., & Lee, Y.-S. (2019). Excitatory

neuron–specific SHP2-ERK signaling network regulates synaptic plasticity and memory. *Science Signaling*, *12*(571), eaau5755. https://doi.org/10.1126/scisignal.aau5755

Saitta, S. C., Harris, S. E., McDonald-McGinn, D. M., Emanuel, B. S., Tonnesen, M. K., Zackai, E. H., Seitz, S. C., & Driscoll, D. A. (2004). Independent de novo 22q11.2 deletions in first cousins with DiGeorge/velocardiofacial syndrome. *American Journal of Medical Genetics*, *124A*(3), 313–317. https://doi.org/10.1002/ajmg.a.20421

Samuels, I. S., Karlo, J. C., Faruzzi, A. N., Pickering, K., Herrup, K., Sweatt, J. D., Saitta, S. C., & Landreth, G. E. (2008). Deletion of ERK2 Mitogen-Activated Protein Kinase Identifies Its Key Roles in Cortical Neurogenesis and Cognitive Function. *Journal of Neuroscience*, *28*(27), 6983–6995. https://doi.org/10.1523/JNEUROSCI.0679-08.2008

Samuels, I. S., Saitta, S. C., & Landreth, G. E. (2009). MAP'ing CNS Development and Cognition: An ERKsome Process. *Neuron*, *61*(2), 160–167. https://doi.org/10.1016/j.neuron.2009.01.001

Sánchez, A. I., García-Acero, M. A., Paredes, A., Quero, R., Ortega, R. I., Rojas, J. A., Herrera, D., Parra, M., Prieto, K., Ángel, J., Rodríguez, L.-S., Prieto, J. C., & Franco, M. (2020). Immunodeficiency in a Patient with 22q11.2 Distal Deletion Syndrome and a p.Ala7dup Variant in the ***MAPK1*** Gene. *Molecular Syndromology*, *11*(1), 15–23. https://doi.org/10.1159/000506032

Sanchez-Ortiz, E., Cho, W., Nazarenko, I., Mo, W., Chen, J., & Parada, L. F. (2014). NF1 regulation of RAS/ERK signaling is required for appropriate granule neuron progenitor expansion and migration in cerebellar development. *Genes & Development*, *28*(21), 2407–2420. https://doi.org/10.1101/gad.246603.114

Sanz, E., Yang, L., Su, T., Morris, D. R., McKnight, G. S., & Amieux, P. S. (2009). Cell-type-specific isolation of ribosome-associated mRNA from complex tissues. *Proceedings of the National Academy of Sciences*, *106*(33), 13939–13944. https://doi.org/10.1073/pnas.0907143106

Selcher, J. C. (2001). Mice Lacking the ERK1 Isoform of MAP Kinase Are Unimpaired in Emotional Learning. *Learning & Memory*, *8*(1), 11–19. https://doi.org/10.1101/lm.37001

Shimamura, K., & Rubenstein, J. L. (1997). Inductive interactions direct early regionalization of the mouse forebrain. *Development*, *124*(14), 2709–2718. https://doi.org/10.1242/dev.124.14.2709

Sik, A., Hajos, N., Gulacsi, A., Mody, I., & Freund, T. F. (1998). The absence of a major Ca2+ signaling pathway in GABAergic neurons of the hippocampus. *Proceedings of the National Academy of Sciences*, *95*(6), 3245–3250. https://doi.org/10.1073/pnas.95.6.3245

Smith, S. J., Sümbül, U., Graybuck, L. T., Collman, F., Seshamani, S., Gala, R., Gliko, O., Elabbady, L., Miller, J. A., Bakken, T. E., Rossier, J., Yao, Z., Lein, E., Zeng, H., Tasic, B., & Hawrylycz, M. (2019). Single-cell transcriptomic evidence for dense intracortical neuropeptide networks. *ELife*, *8*, e47889. https://doi.org/10.7554/eLife.47889

Song, Y.-H., Hwang, Y.-S., Kim, K., Lee, H.-R., Kim, J.-H., Maclachlan, C., Dubois, A., Jung, M. W., Petersen, C. C. H., Knott, G., Lee, S.-H., & Lee, S.-H. (2020). Somatostatin enhances visual processing and perception by suppressing excitatory inputs to parvalbumin-positive interneurons in V1. *Science Advances*, *6*(17), eaaz0517. https://doi.org/10.1126/sciadv.aaz0517

Song, Y.-H., Yoon, J., & Lee, S.-H. (2021). The role of neuropeptide somatostatin in the brain and its application in treating neurological disorders. *Experimental & Molecular Medicine*, *53*(3), 328–338. https://doi.org/10.1038/s12276-021-00580-4

Southwell, D. G., Paredes, M. F., Galvao, R. P., Jones, D. L., Froemke, R. C., Sebe, J. Y., Alfaro-Cervello, C., Tang, Y., Garcia-Verdugo, J. M., Rubenstein, J. L., Baraban, S. C., & Alvarez-Buylla, A. (2012). Intrinsically determined cell death of developing cortical interneurons. *Nature*, *491*(7422), 109–113. https://doi.org/10.1038/nature11523

Spiegel, I., Mardinly, A. R., Gabel, H. W., Bazinet, J. E., Couch, C. H., Tzeng, C. P., Harmin, D. A., & Greenberg, M. E. (2014). Npas4 Regulates Excitatory-Inhibitory Balance within Neural Circuits through Cell-Type-Specific Gene Programs. *Cell*, *157*(5), 1216–1229. https://doi.org/10.1016/j.cell.2014.03.058

Sun, Y., Qian, L., Xu, L., Hunt, S., & Sah, P. (2020). Somatostatin neurons in the central amygdala mediate anxiety by disinhibition of the central sublenticular extended amygdala. *Molecular Psychiatry*. https://doi.org/10.1038/s41380-020-00894-1

Talley, M. J., Nardini, D., Qin, S., Prada, C. E., Ehrman, L. A., & Waclaw, R. R. (2021). A role for sustained MAPK activity in the mouse ventral telencephalon. *Developmental Biology*, *476*, 137–147. https://doi.org/10.1016/j.ydbio.2021.03.019

Taniguchi, H., He, M., Wu, P., Kim, S., Paik, R., Sugino, K., Kvitsani, D., Fu, Y., Lu, J., Lin, Y., Miyoshi, G., Shima, Y., Fishell, G., Nelson, S. B., & Huang, Z. J. (2011). A Resource of Cre Driver Lines for Genetic Targeting of GABAergic Neurons in Cerebral Cortex. *Neuron*, *71*(6), 995–1013. https://doi.org/10.1016/j.neuron.2011.07.026

Tasic, B., Menon, V., Nguyen, T. N., Kim, T. K., Jarsky, T., Yao, Z., Levi, B., Gray, L. T., Sorensen, S. A., Dolbeare, T., Bertagnolli, D., Goldy, J., Shapovalova, N., Parry, S., Lee, C., Smith, K., Bernard, A., Madisen, L., Sunkin, S. M., … Zeng, H. (2016). Adult mouse cortical cell taxonomy revealed by single cell transcriptomics. *Nature Neuroscience*, *19*(2), 335–346. https://doi.org/10.1038/nn.4216

Tereshko, L., Gao, Y., Cary, B. A., Turrigiano, G. G., & Sengupta, P. (2021). Ciliary neuropeptidergic signaling dynamically regulates excitatory synapses in postnatal neocortical pyramidal neurons. *ELife*, *10*, e65427. https://doi.org/10.7554/eLife.65427

Thomas, G. M., & Huganir, R. L. (2004). MAPK cascade signalling and synaptic plasticity. *Nature Reviews Neuroscience*, *5*(3), 173–183. https://doi.org/10.1038/nrn1346

Tidyman, W. E., & Rauen, K. A. (2016). Pathogenetics of the RASopathies. *Human Molecular Genetics*, *25*(R2), R123–R132. https://doi.org/10.1093/hmg/ddw191

Ting, A. K., Chen, Y., Wen, L., Yin, D.-M., Shen, C., Tao, Y., Liu, X., Xiong, W.-C., & Mei, L. (2011). Neuregulin 1 Promotes Excitatory Synapse Development and Function in GABAergic Interneurons. *Journal of Neuroscience*, *31*(1), 15–25. https://doi.org/10.1523/JNEUROSCI.2538-10.2011

Topolnik, L. (2012). Dendritic calcium mechanisms and long-term potentiation in cortical inhibitory interneurons: Calcium in interneuron dendrites. *European Journal of Neuroscience*, *35*(4), 496–506. https://doi.org/10.1111/j.1460-9568.2011.07988.x

Topolnik, L., Azzi, M., Morin, F., Kougioumoutzakis, A., & Lacaille, J.-C. (2006). mGluR1/5 subtype-specific calcium signalling and induction of long-term potentiation in rat hippocampal oriens/alveus interneurones: MGluR1/5 Ca^{2+} signalling and LTP in interneurones. *The Journal of Physiology*, *575*(1), 115–131. https://doi.org/10.1113/jphysiol.2006.112896

Tripp, A., Kota, R. S., Lewis, D. A., & Sibille, E. (2011). Reduced somatostatin in subgenual anterior cingulate cortex in major depression. *Neurobiology of Disease*, *42*(1), 116–124. https://doi.org/10.1016/j.nbd.2011.01.014

Tucker, E. S., Segall, S., Gopalakrishna, D., Wu, Y., Vernon, M., Polleux, F., & LaMantia, A.-S. (2008). Molecular Specification and Patterning of Progenitor Cells in the Lateral and Medial Ganglionic Eminences. *Journal of Neuroscience*, *28*(38), 9504–9518. https://doi.org/10.1523/JNEUROSCI.2341-08.2008

Tuncdemir, S. N., Wamsley, B., Stam, F. J., Osakada, F., Goulding, M., Callaway, E. M., Rudy, B., & Fishell, G. (2016). Early Somatostatin Interneuron Connectivity Mediates the Maturation of Deep Layer Cortical Circuits. *Neuron*, *89*(3), 521–535. https://doi.org/10.1016/j.neuron.2015.11.020

Tyson, J. A., Goldberg, E. M., Maroof, A. M., Xu, Q., Petros, T. J., & Anderson, S. A. (2015). Duration of culture and sonic hedgehog signaling differentially specify PV versus SST cortical interneuron fates from embryonic stem cells. *Development*, *142*(7), 1267–1278. https://doi.org/10.1242/dev.111526

Urban-Ciecko, J., & Barth, A. L. (2016). Somatostatin-expressing neurons in cortical networks. *Nature Reviews Neuroscience*, *17*(7), 401–409. https://doi.org/10.1038/nrn.2016.53

Vithayathil, J., Pucilowska, J., Goodnough, L. H., Atit, R. P., & Landreth, G. E. (2015). Dentate Gyrus Development Requires ERK Activity to Maintain Progenitor Population and MAPK Pathway

Feedback Regulation. *Journal of Neuroscience*, *35*(17), 6836–6848. https://doi.org/10.1523/JNEUROSCI.4196-14.2015

Vogt, D., Cho, K. K. A., Lee, A. T., Sohal, V. S., & Rubenstein, J. L. R. (2015). The Parvalbumin/Somatostatin Ratio Is Increased in Pten Mutant Mice and by Human PTEN ASD Alleles. *Cell Reports*, *11*(6), 944–956. https://doi.org/10.1016/j.celrep.2015.04.019

Vong, L., Ye, C., Yang, Z., Choi, B., Chua, S., & Lowell, B. B. (2011). Leptin Action on GABAergic Neurons Prevents Obesity and Reduces Inhibitory Tone to POMC Neurons. *Neuron*, *71*(1), 142–154. https://doi.org/10.1016/j.neuron.2011.05.028

Wei, Y., Han, X., & Zhao, C. (2020). PDK1 regulates the survival of the developing cortical interneurons. *Molecular Brain*, *13*(1), 65. https://doi.org/10.1186/s13041-020-00604-6

Wengert, E. R., Miralles, R. M., Wedgwood, K. C. A., Wagley, P. K., Strohm, S. M., Panchal, P. S., Idrissi, A. M., Wenker, I. C., Thompson, J. A., Gaykema, R. P., & Patel, M. K. (2021). Somatostatin-Positive Interneurons Contribute to Seizures in SCN8A Epileptic Encephalopathy. *The Journal of Neuroscience*, *41*(44), 9257–9273. https://doi.org/10.1523/JNEUROSCI.0718-21.2021

Wonders, C. P., & Anderson, S. A. (2006). The origin and specification of cortical interneurons. *Nature Reviews Neuroscience*, *7*(9), 687–696. https://doi.org/10.1038/nrn1954

Wong, F. K., Bercsenyi, K., Sreenivasan, V., Portalés, A., Fernández-Otero, M., & Marín, O. (2018). Pyramidal cell regulation of interneuron survival sculpts cortical networks. *Nature*, *557*(7707), 668–673. https://doi.org/10.1038/s41586-018-0139-6

Wu, G.-Y., Deisseroth, K., & Tsien, R. W. (2001). Activity-dependent CREB phosphorylation: Convergence of a fast, sensitive calmodulin kinase pathway and a slow, less sensitive mitogen-activated protein kinase pathway. *Proceedings of the National Academy of Sciences*, *98*(5), 2808–2813. https://doi.org/10.1073/pnas.051634198

Xing, J., Ginty, D. D., & Greenberg, M. E. (1996). Coupling of the RAS-MAPK Pathway to Gene Activation by RSK2, a Growth Factor-Regulated CREB Kinase. *Science*, *273*(5277), 959–963. https://doi.org/10.1126/science.273.5277.959

Xing, L., Larsen, R. S., Bjorklund, G. R., Li, X., Wu, Y., Philpot, B. D., Snider, W. D., & Newbern, J. M. (2016). Layer specific and general requirements for ERK/MAPK signaling in the developing neocortex. *ELife*, *5*, e11123. https://doi.org/10.7554/eLife.11123

Xu, Q., Guo, L., Moore, H., Waclaw, R. R., Campbell, K., & Anderson, S. A. (2010). Sonic Hedgehog Signaling Confers Ventral Telencephalic Progenitors with Distinct Cortical Interneuron Fates. *Neuron*, *65*(3), 328–340. https://doi.org/10.1016/j.neuron.2010.01.004

Xu, Q., Tam, M., & Anderson, S. A. (2008). Fate mapping Nkx2.1-lineage cells in the mouse telencephalon. *The Journal of Comparative Neurology*, *506*(1), 16–29. https://doi.org/10.1002/cne.21529

Xu, Q., Wonders, C. P., & Anderson, S. A. (2005). Sonic hedgehog maintains the identity of cortical interneuron progenitors in the ventral telencephalon. *Development*, *132*(22), 4987–4998. https://doi.org/10.1242/dev.02090

Yamamoto, K. K., Gonzalez, G. A., Biggs, W. H., & Montminy, M. R. (1988). Phosphorylation-induced binding and transcriptional efficacy of nuclear factor CREB. *Nature*, *334*(6182), 494–498. https://doi.org/10.1038/334494a0

Yap, E.-L., & Greenberg, M. E. (2018). Activity-Regulated Transcription: Bridging the Gap between Neural Activity and Behavior. *Neuron*, *100*(2), 330–348. https://doi.org/10.1016/j.neuron.2018.10.013

Yu, W., Wang, Y., McDonnell, K., Stephen, D., & Bai, C. B. (2009). Patterning of ventral telencephalon requires positive function of Gli transcription factors. *Developmental Biology*, *334*(1), 264–275. https://doi.org/10.1016/j.ydbio.2009.07.026

Zhu, H., Aryal, D. K., Olsen, R. H. J., Urban, D. J., Swearingen, A., Forbes, S., Roth, B. L., & Hochgeschwender, U. (2016). Cre-dependent DREADD (Designer Receptors Exclusively

Activated by Designer Drugs) mice. *Genesis (New York, N.Y.: 2000)*, *54*(8), 439–446. https://doi.org/10.1002/dvg.22949

Zou, D., Chen, L., Deng, D., Jiang, D., Dong, F., McSweeney, C., Zhou, Y., Liu, L., Chen, G., Wu, Y., & Mao, Y. (2016). DREADD in Parvalbumin Interneurons of the Dentate Gyrus Modulates Anxiety, Social Interaction and Memory Extinction. *Current Molecular Medicine*, *16*(1), 91–102. https://doi.org/10.2174/1566524016666151222150024

Figure 1

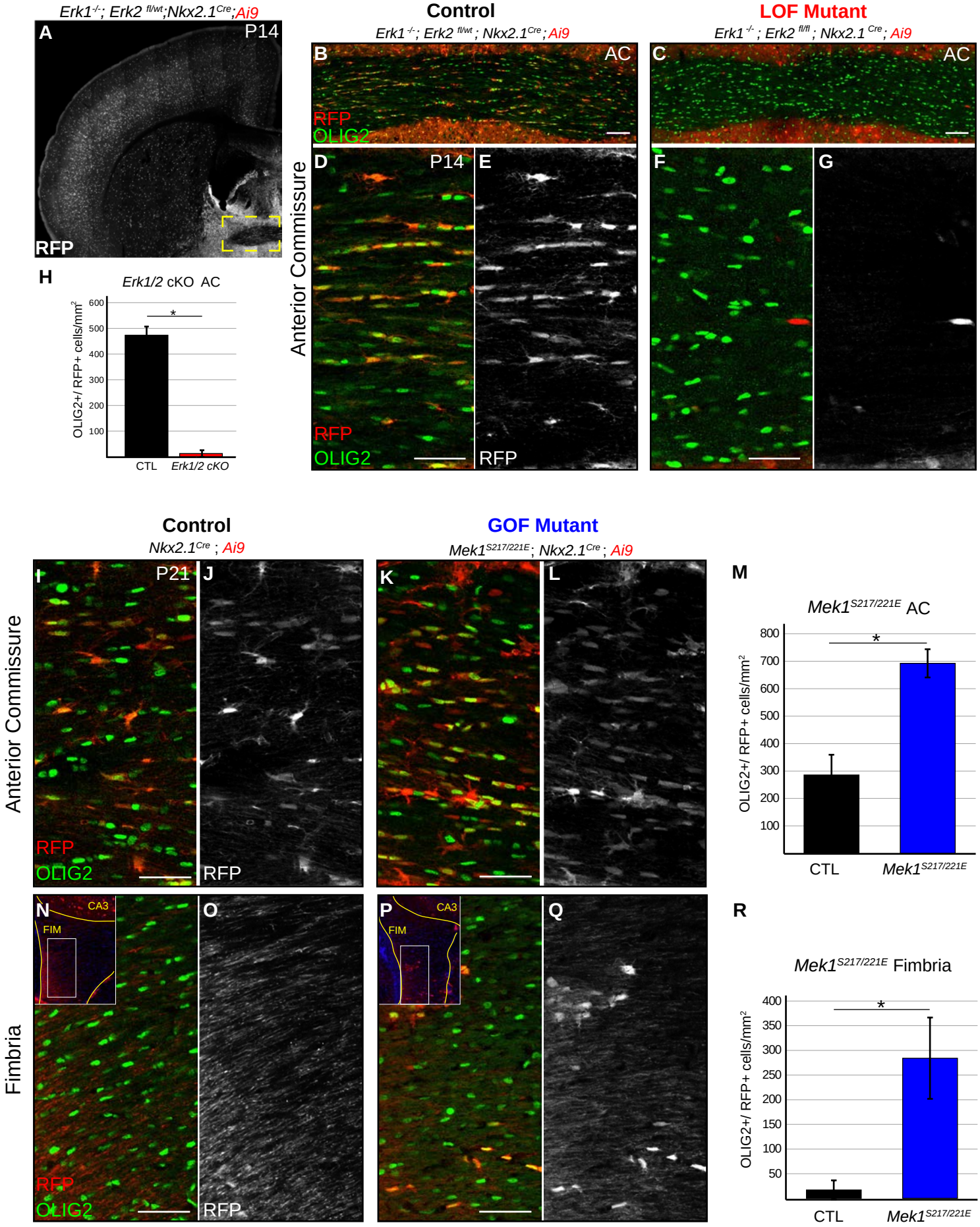
Erk1-/-; Erk2 fl/wt;Nkx2.1Cre;Ai9
A
P14
RFP
H
Erk1/2 cKO AC
OLIG2+/ RFP+ cells/mm2
600
500
400
300
200
100
*
CTL
Erk1/2 cKO
Control
Erk1-/-; Erk2 fl/wt; Nkx2.1Cre; Ai9
LOF Mutant
Erk1-/-; Erk2 fl/fl; Nkx2.1Cre; Ai9
Anterior Commissure
B
AC
RFP
OLIG2
C
AC
D
P14
E
RFP
OLIG2
RFP
F
G
Control
Nkx2.1Cre ; Ai9
GOF Mutant
Mek1S217/221E; Nkx2.1Cre; Ai9
Anterior Commissure
I
P21
J
RFP
OLIG2
RFP
K
L
M
Mek1S217/221E AC
OLIG2+/ RFP+ cells/mm2
800
700
600
500
400
300
200
100
*
CTL
Mek1S217/221E
Fimbria
N
CA3
FIM
O
RFP
OLIG2
RFP
P
CA3
FIM
Q
R
Mek1S217/221E Fimbria
OLIG2+/ RFP+ cells/mm2
400
350
300
250
200
150
100
50
*
CTL
Mek1S217/221E

Nkx2.1^{Cre}, Ai9

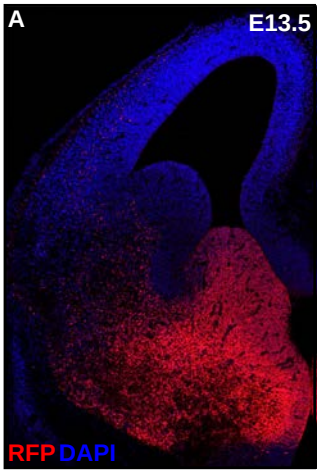

B

OLIG2+ Cells in Anterior Commissure							
Age	**Genotype**	**N**	**Area sampled (mm²)**	**Total OLIG2+ cells counted**	**OLIG2+ cells/mm²**	**Total RFP+/OLIG2+ cells counted**	**% RFP+**
P14	*Erk1$^{-/-}$, Erk2$^{fl/wt}$, Nkx2.1^{Cre}, Ai9*	3	0.118	117	1497 +/- 39	56	**31.60**
P14	*Erk1$^{-/-}$, Erk2$^{fl/fl}$, Nkx2.1^{Cre}, Ai9*	3	0.237	336	1420 +/- 133	3	**0.92**
P21	*Nkx2.1 Cre, Ai9*	4	3.24	649	2077 +/- 164	98	**13.72**
P21	*MEK1$^{S217/221E}$, Nkx2.1^{Cre}, Ai9*	4	4.45	1042	2385 +/- 92	311	**29.01**

Erk1/2, Nkx2.1^{Cre}, Ai9

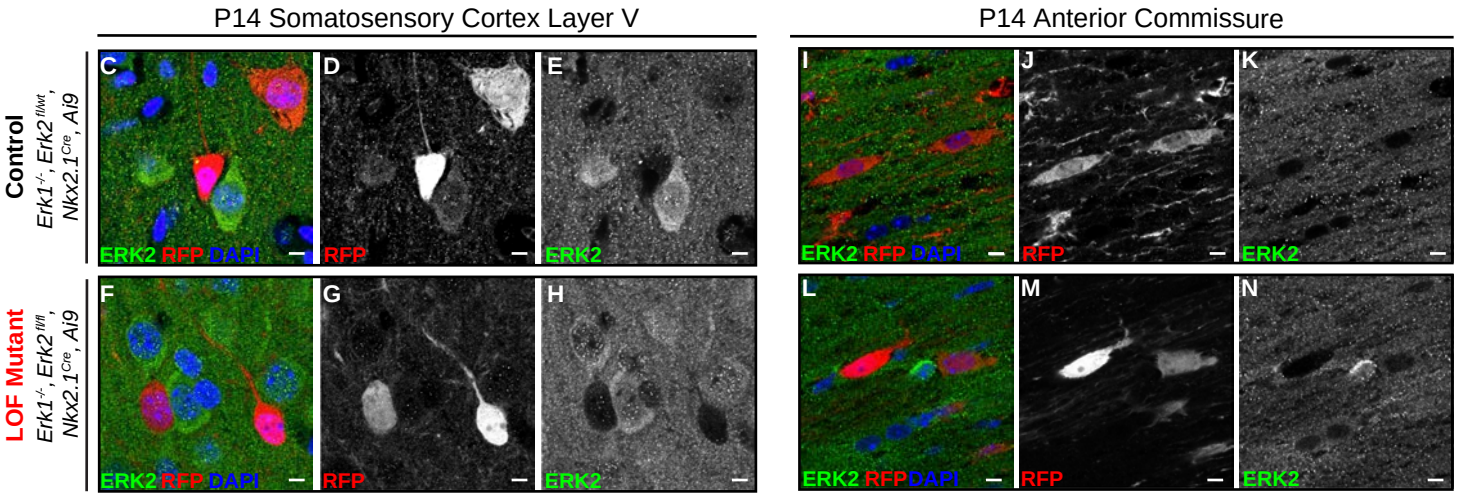

Mek1$^{S217/221E}$, Nkx2.1^{Cre}, Ai9

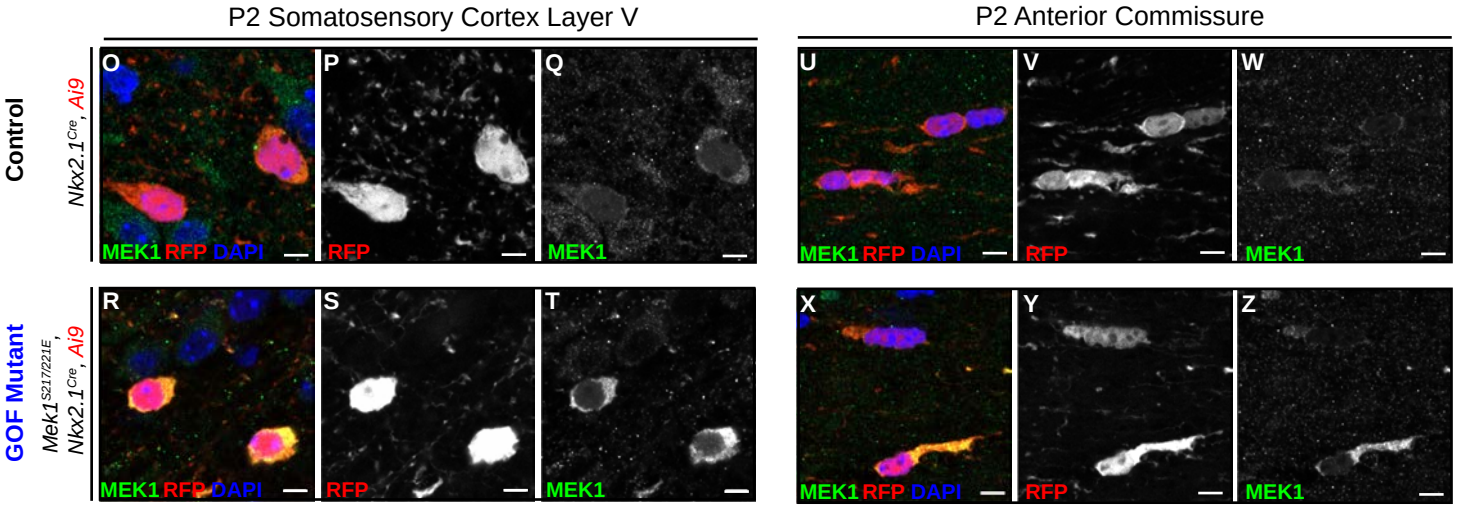

Figure 2

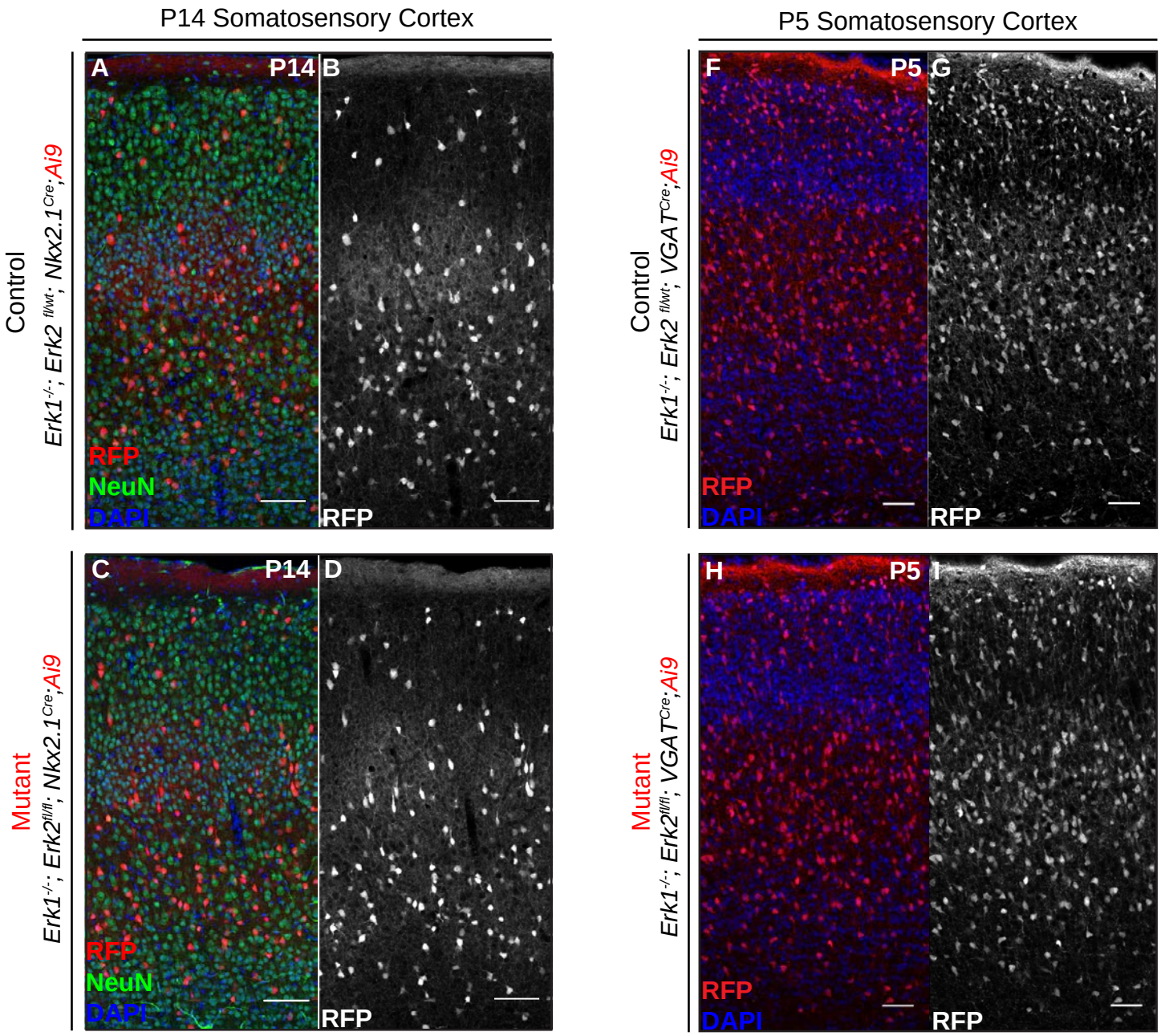
P14 Somatosensory Cortex
P5 Somatosensory Cortex
Control
Erk1-/-; Erk2 fl/wt; Nkx2.1Cre;Ai9
Control
Erk1-/-; Erk2 fl/wt; VGATCre;Ai9
Mutant
Erk1-/-; Erk2fl/fl; Nkx2.1Cre;Ai9
Mutant
Erk1-/-; Erk2fl/fl; VGATCre;Ai9
A
P14
B
C
P14
D
F
P5
G
H
P5
I
RFP
NeuN
DAPI
RFP

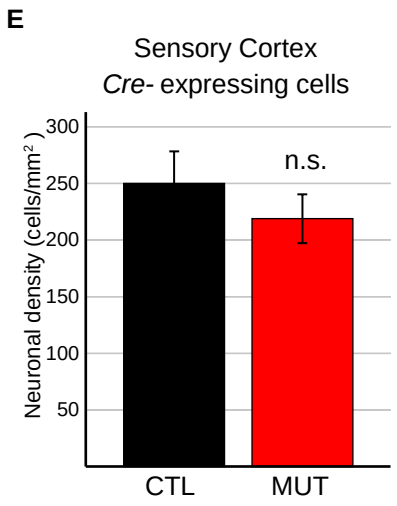
E
Sensory Cortex
Cre- expressing cells
Neuronal density (cells/mm2)
300
250
200
150
100
50
n.s.
CTL
MUT

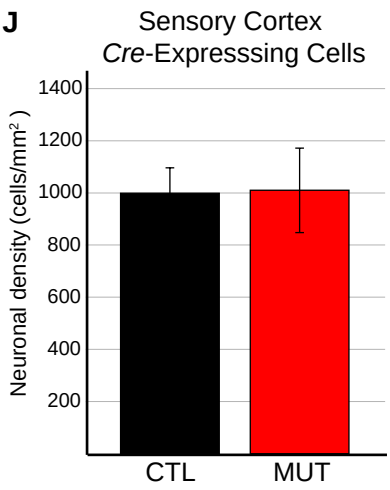
J
Sensory Cortex
Cre-Expresssing Cells
Neuronal density (cells/mm2)
1400
1200
1000
800
600
400
200
CTL
MUT

Figure 2 - figure supplement 1

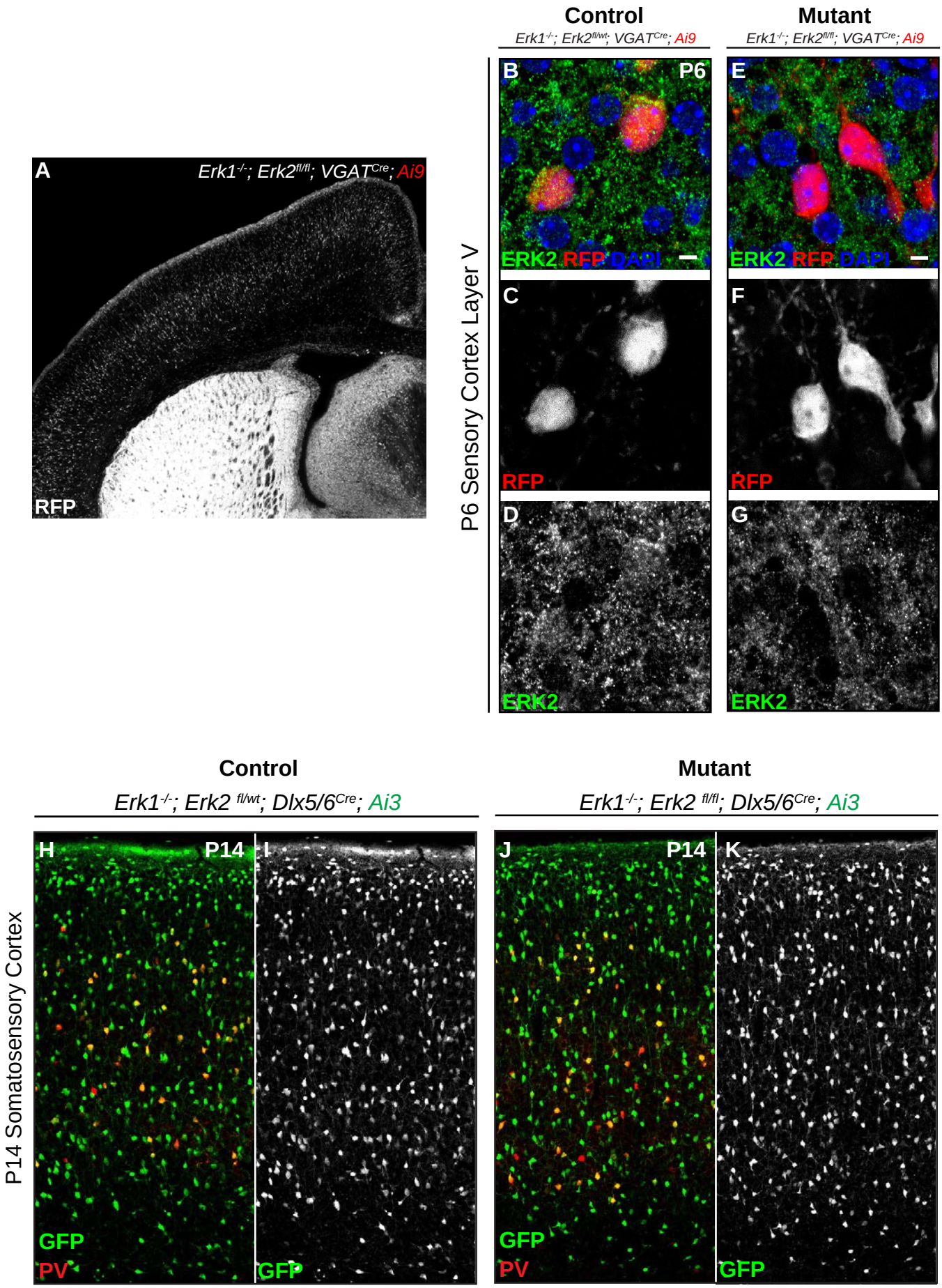

Figure 3

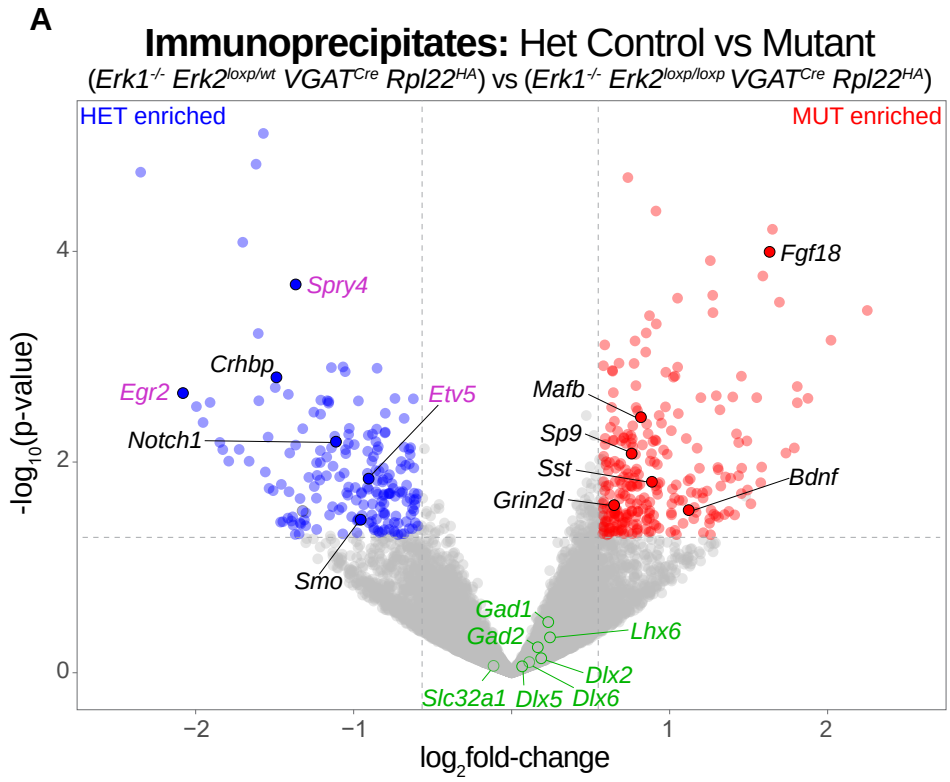
A
Immunoprecipitates: Het Control vs Mutant
(Erk1-/- Erk2loxp/wt VGATCre Rpl22HA) vs (Erk1-/- Erk2loxp/loxp VGATCre Rpl22HA)
HET enriched
MUT enriched
Spry4
Crhbp
Egr2
Notch1
Etv5
Smo
Fgf18
Mafb
Sp9
Sst
Grin2d
Bdnf
Gad1
Gad2
Lhx6
Dlx2
Slc32a1
Dlx5
Dlx6
-log10(p-value)
log2fold-change

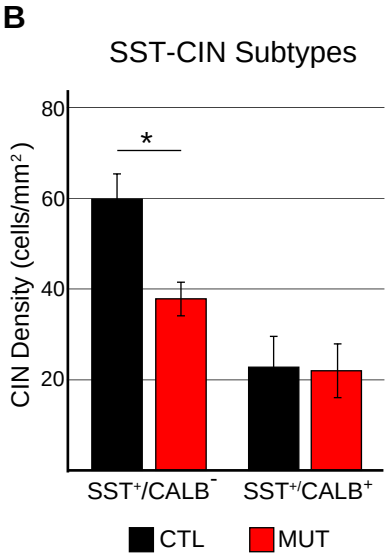
B
SST-CIN Subtypes
CIN Density (cells/mm2)
SST+/CALB-
SST+/CALB+
CTL
MUT

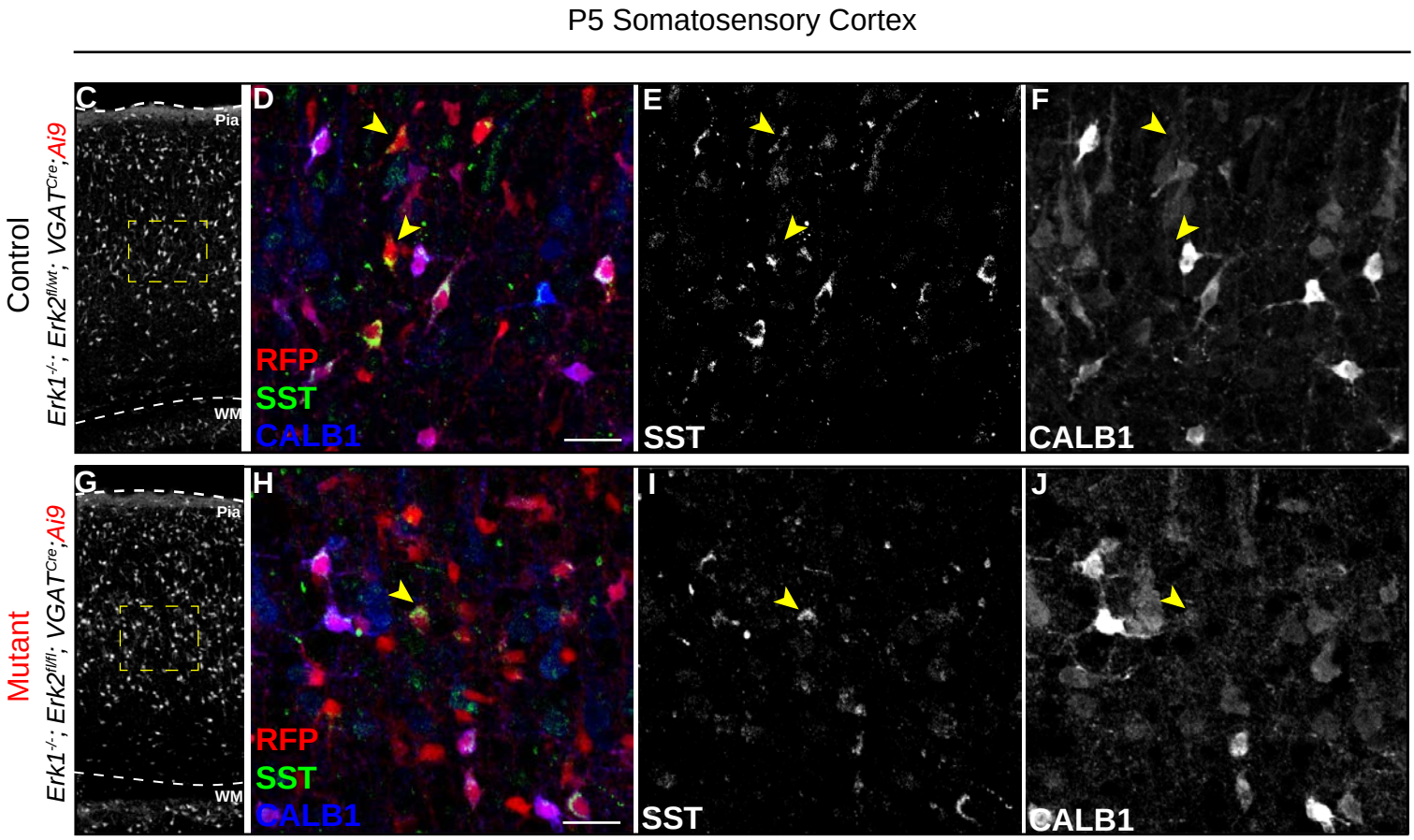
P5 Somatosensory Cortex
Control
Erk1-/-; Erk2fl/wt; VGATCre;Ai9
Mutant
Erk1-/-; Erk2fl/fl; VGATCre;Ai9
Pia
WM
RFP
SST
CALB1

Figure 3 - figure supplement 1

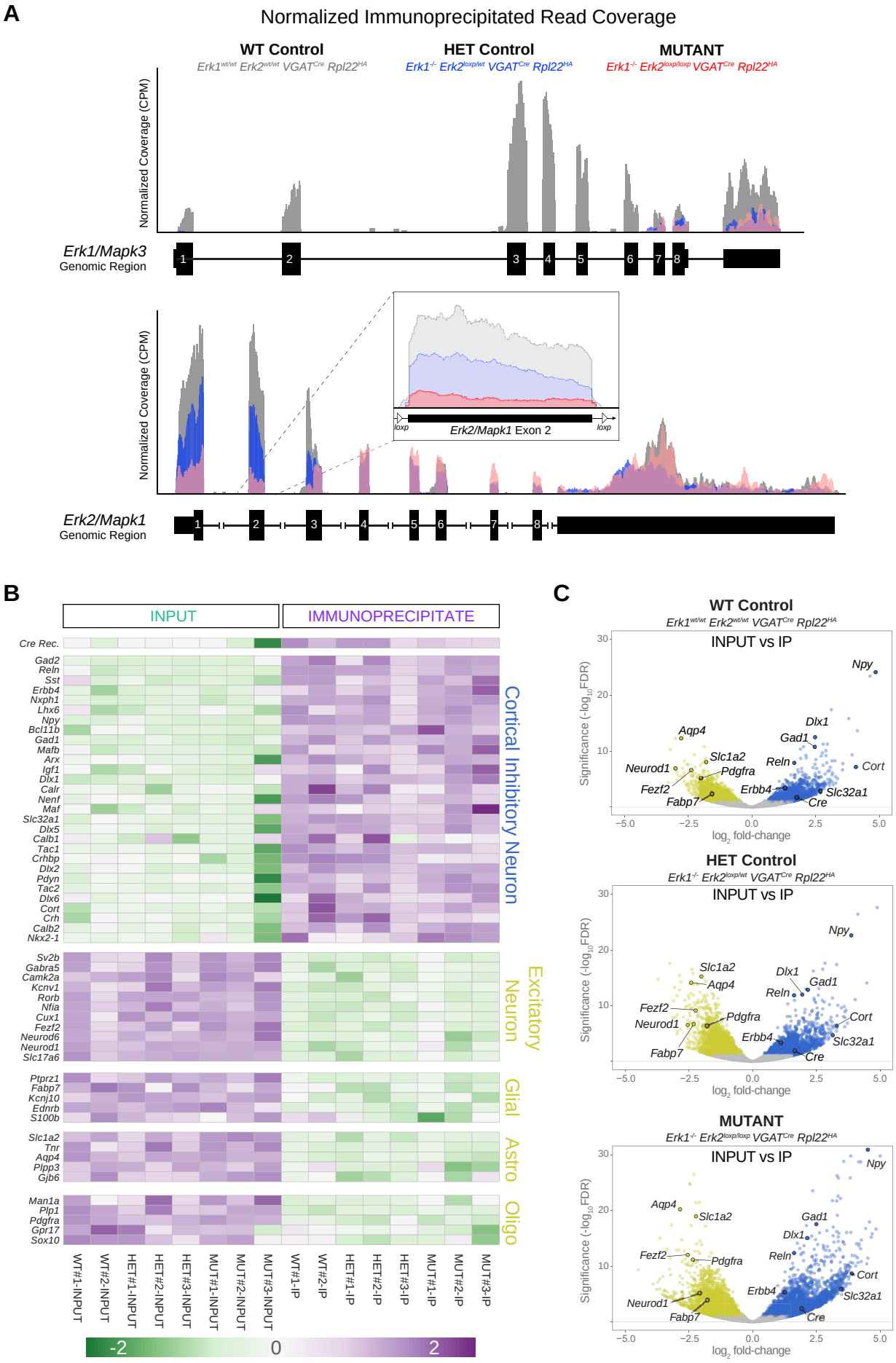

Figure 4

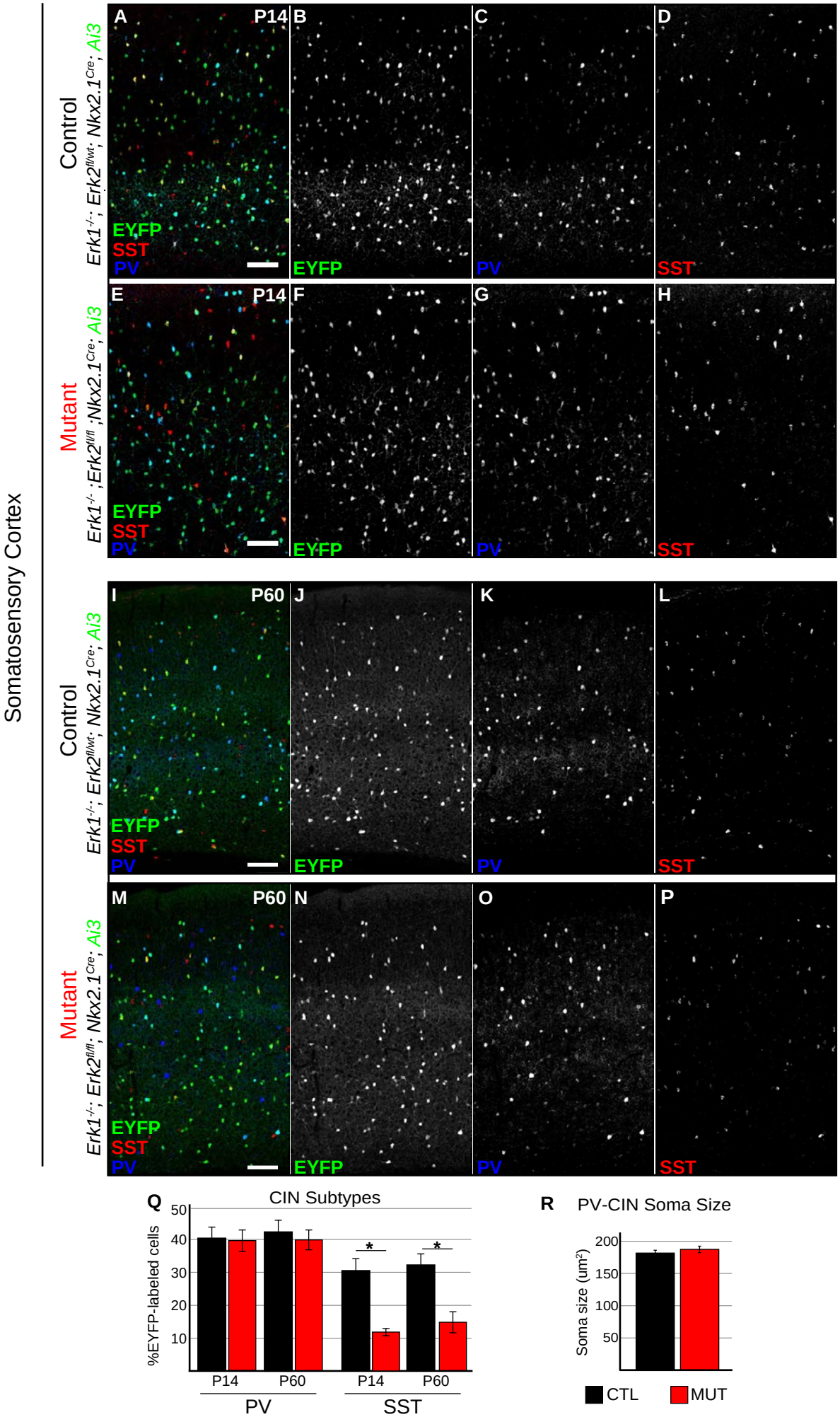
Somatosensory Cortex
Control
Erk1-/-; Erk2fl/wt; Nkx2.1Cre; Ai3
Mutant
Erk1-/-; Erk2fl/fl; Nkx2.1Cre; Ai3
A
P14
B
C
D
E
P14
F
G
H
I
P60
J
K
L
M
P60
N
O
P
EYFP
SST
PV
Q
CIN Subtypes
%EYFP-labeled cells
50
40
30
20
10
*
*
P14
P60
P14
P60
PV
SST
R
PV-CIN Soma Size
Soma size (um2)
200
150
100
50
CTL
MUT

Figure 4 - figure supplement 1

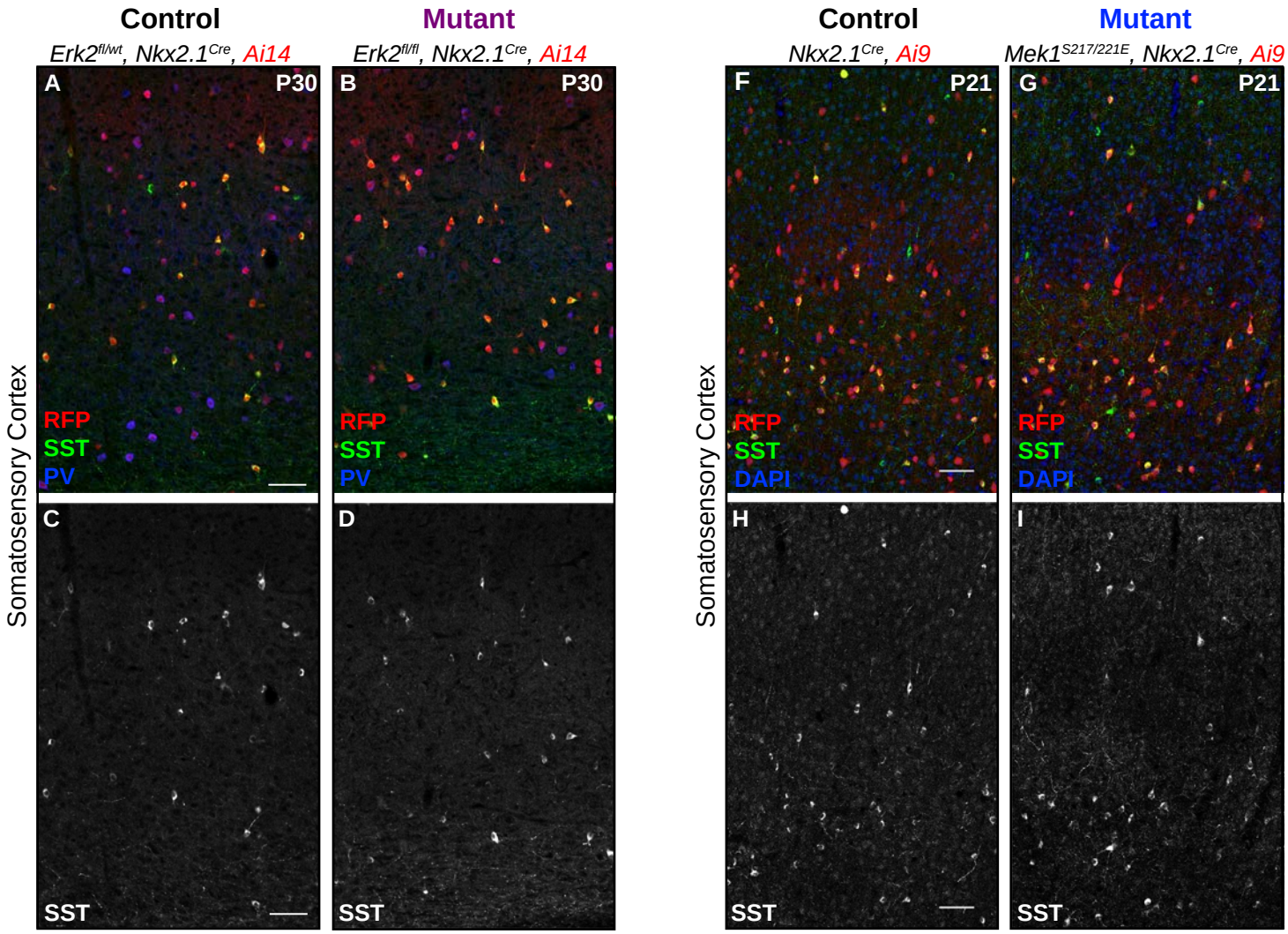

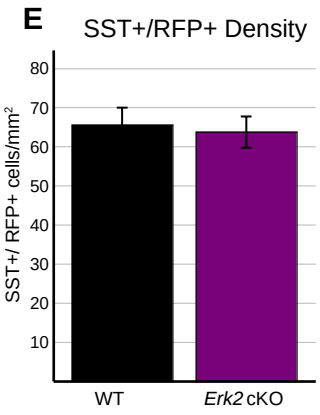

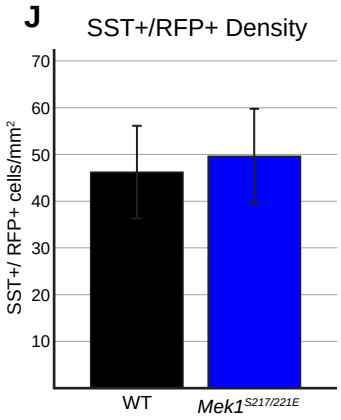

Figure 5

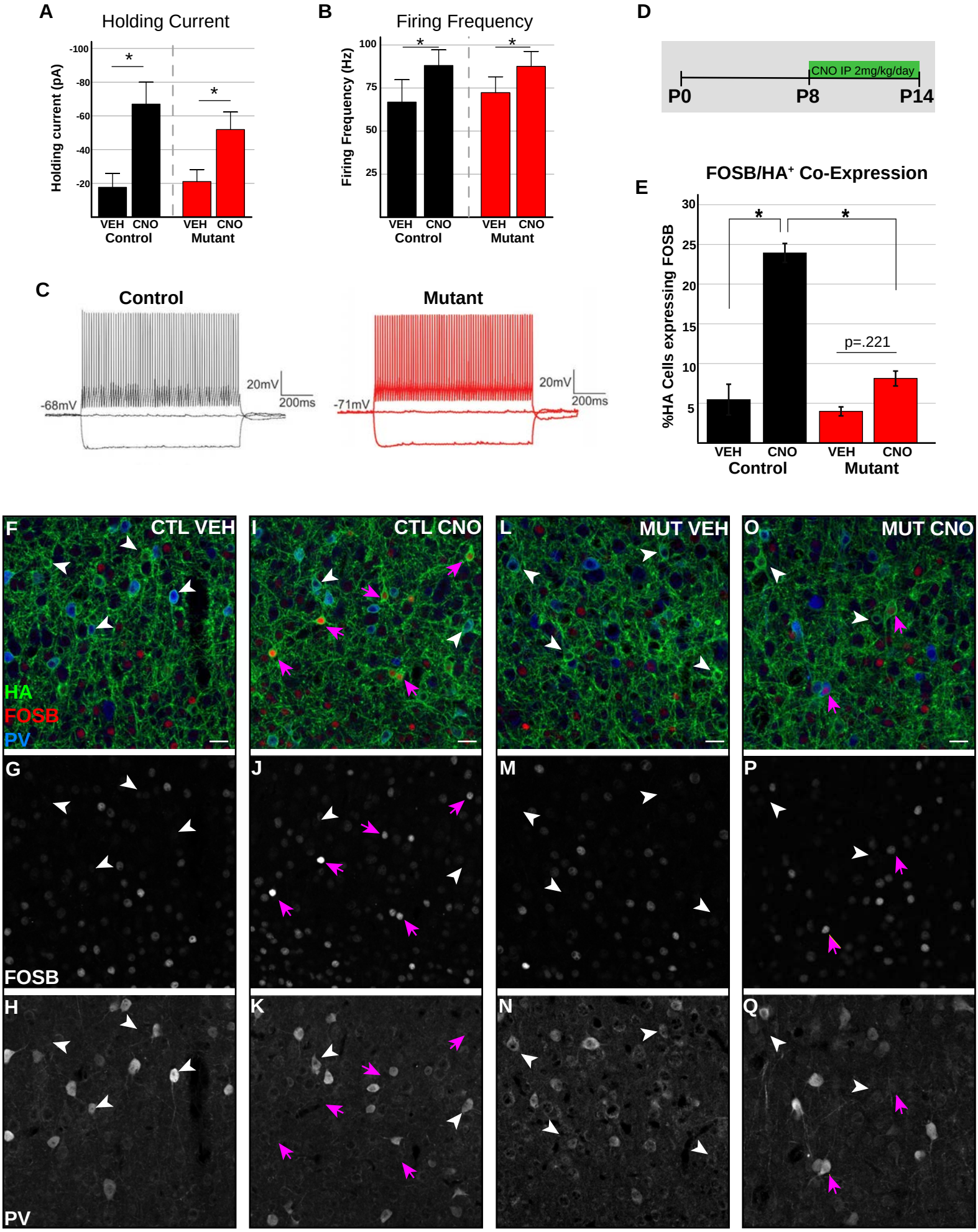
A
Holding Current
Holding current (pA)
-100
-80
-60
-40
-20
*
*
VEH CNO VEH CNO
Control Mutant
B
Firing Frequency
Firing Frequency (Hz)
100
75
50
25
*
*
VEH CNO VEH CNO
Control Mutant
D
CNO IP 2mg/kg/day
P0
P8
P14
C
Control
Mutant
-68mV
20mV
200ms
-71mV
20mV
200ms
E
FOSB/HA+ Co-Expression
%HA Cells expressing FOSB
30
25
20
15
10
5
*
*
p=.221
VEH CNO VEH CNO
Control Mutant
F
CTL VEH
HA
FOSB
PV
I
CTL CNO
L
MUT VEH
O
MUT CNO
G
FOSB
J
M
P
H
PV
K
N
Q

Figure 5 - figure supplement 1

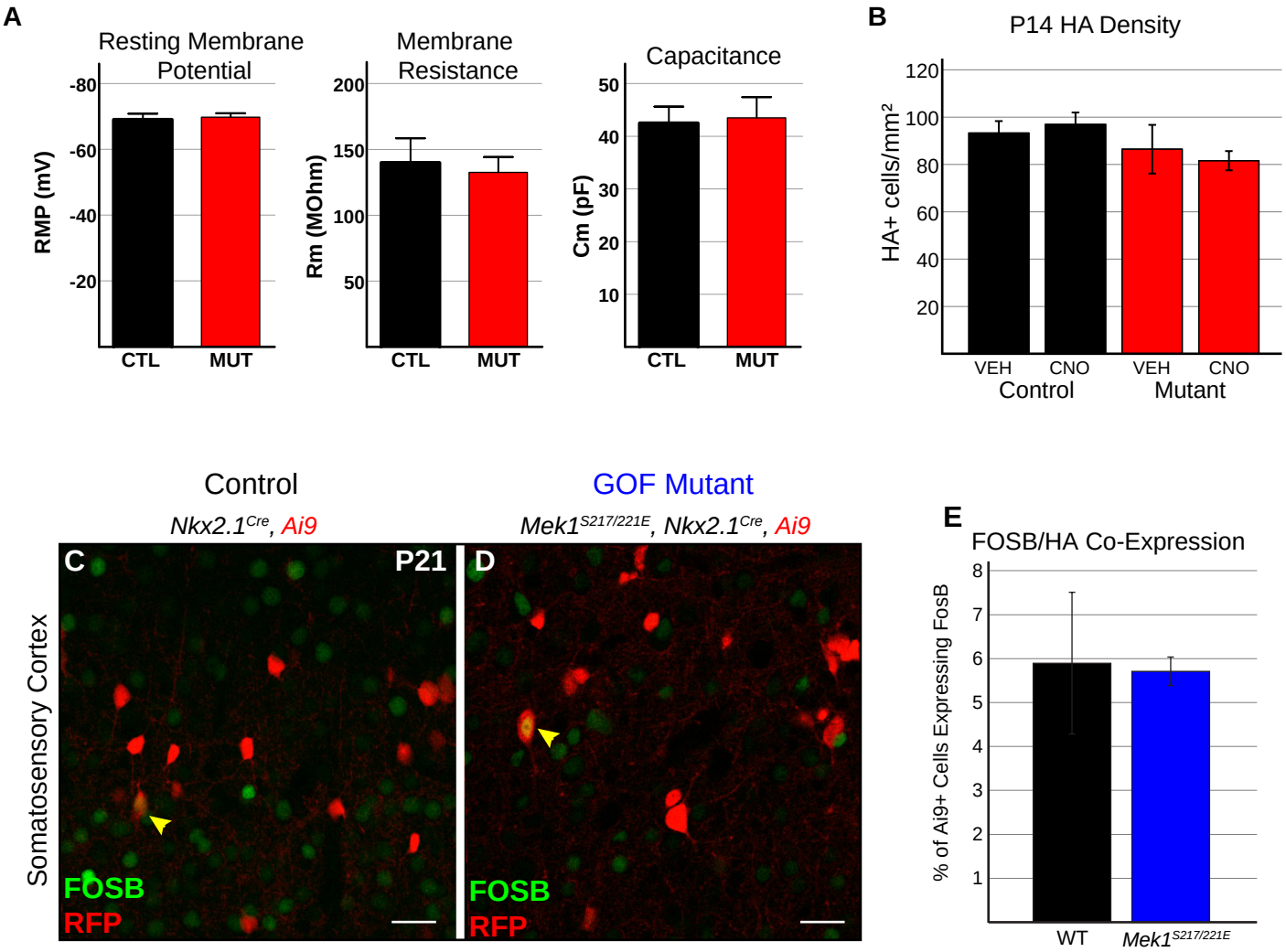

Figure 6

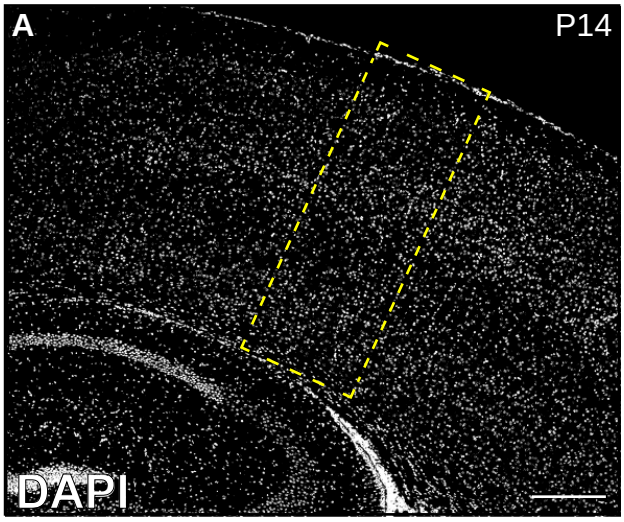
A
P14
DAPI

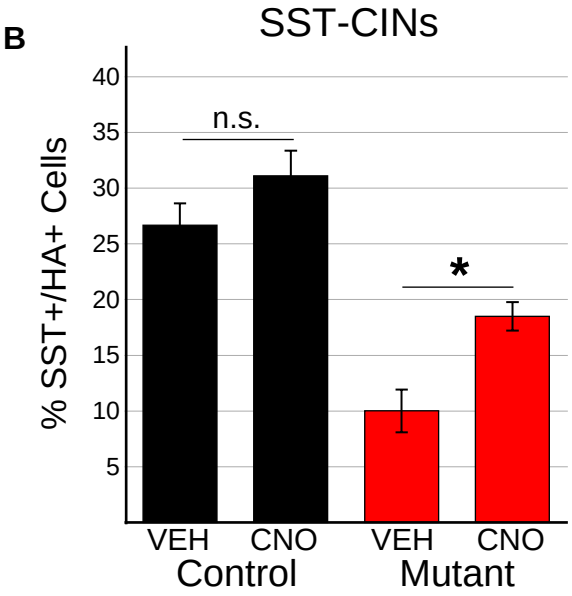
B
SST-CINs
% SST+/HA+ Cells
40
35
30
25
20
15
10
5
n.s.
*
VEH
CNO
VEH
CNO
Control
Mutant

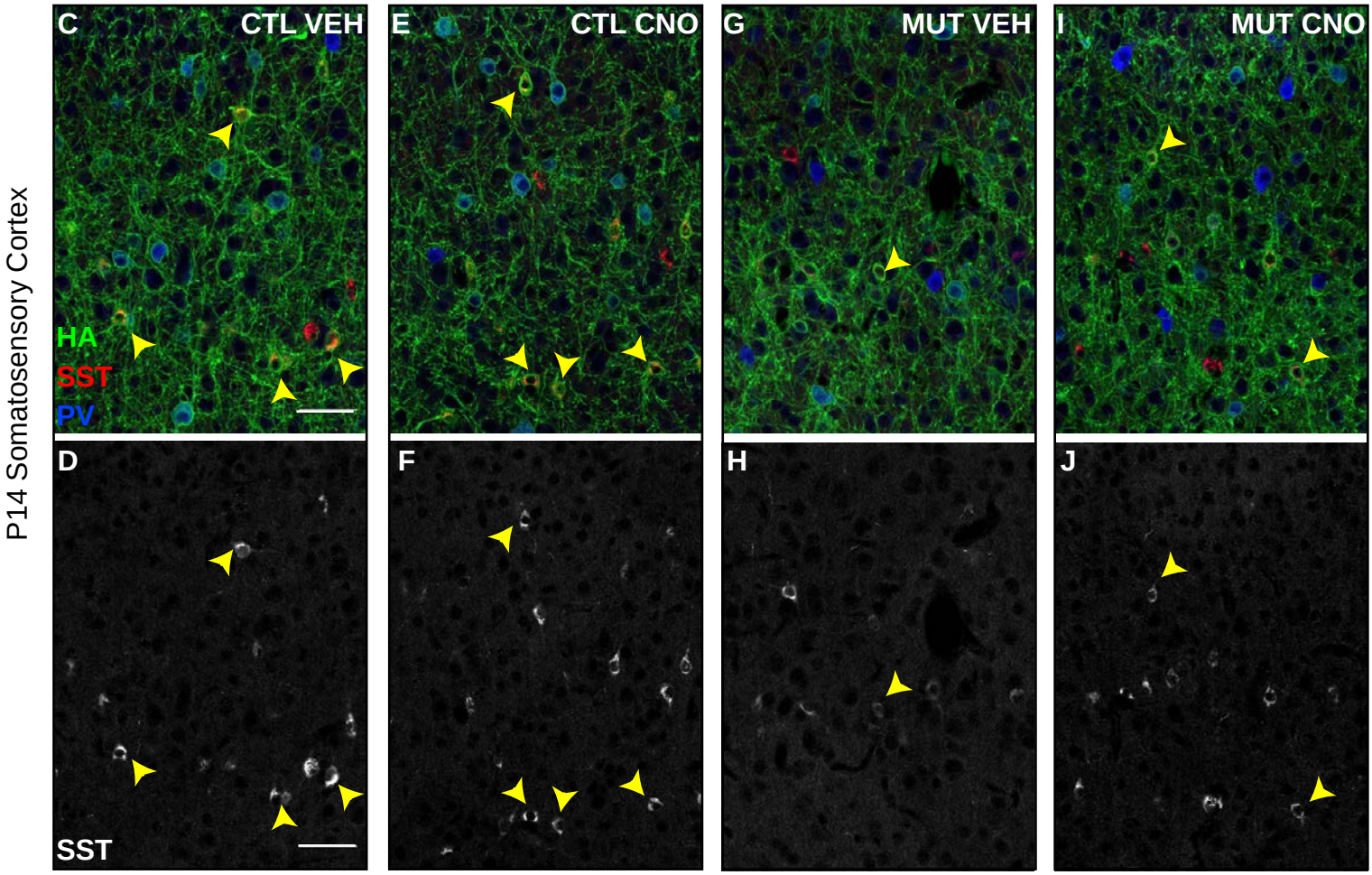
P14 Somatosensory Cortex
C
CTL VEH
HA
SST
PV
E
CTL CNO
G
MUT VEH
I
MUT CNO
D
SST
F
H
J

Figure 7

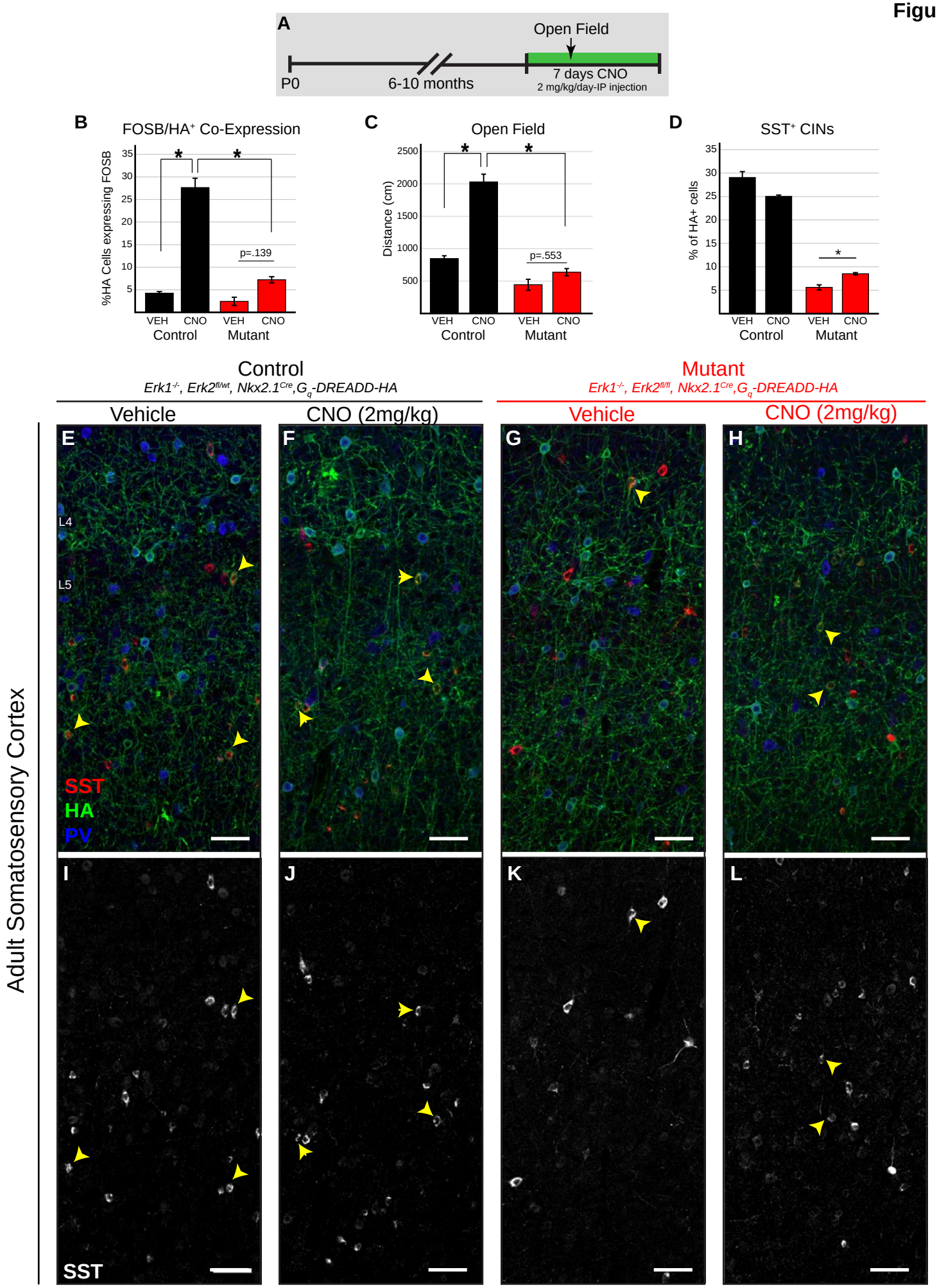
A
Open Field
P0
6-10 months
7 days CNO
2 mg/kg/day-IP injection
B
FOSB/HA+ Co-Expression
%HA Cells expressing FOSB
p=.139
VEH CNO VEH CNO
Control Mutant
C
Open Field
Distance (cm)
p=.553
VEH CNO VEH CNO
Control Mutant
D
SST+ CINs
% of HA+ cells
VEH CNO VEH CNO
Control Mutant
Control
Erk1-/-, Erk2fl/wt, Nkx2.1Cre,Gq-DREADD-HA
Mutant
Erk1-/-, Erk2fl/fl, Nkx2.1Cre,Gq-DREADD-HA
Vehicle
CNO (2mg/kg)
Vehicle
CNO (2mg/kg)
Adult Somatosensory Cortex
E
F
G
H
L4
L5
SST
HA
PV
I
J
K
L
SST
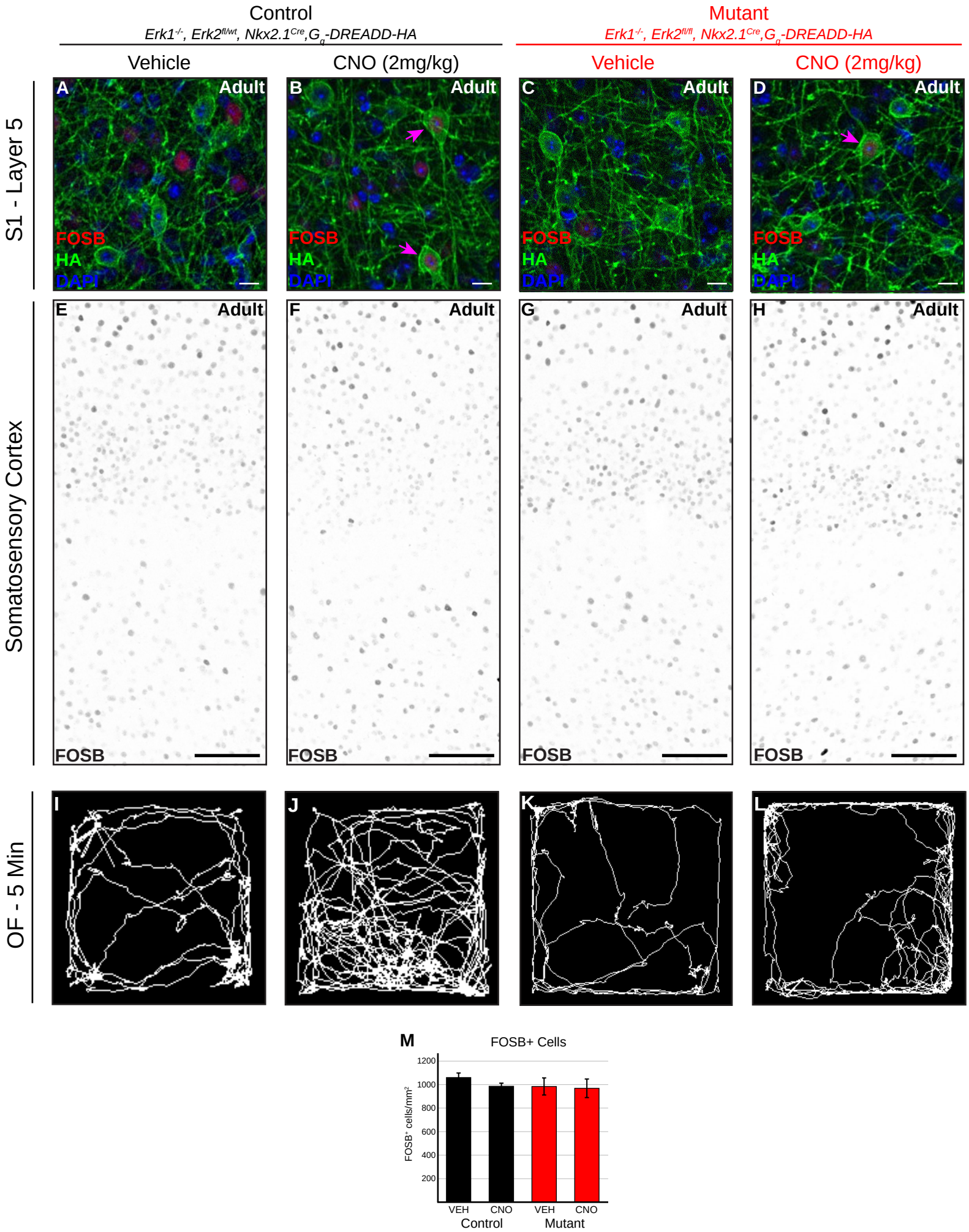
Figure 7 - figure supplement 1